BROADENING OF THE POTASSIUM RESONANCE LINES FOR HIGH PRESSURES OF A HOMOGENEOUS ABSORBING VAPOR

Thesis

by

Paul E Lloyd

In partial fulfilment of the requirements

for the degree of Doctor of Philosophy

CALIFORNIA INSTITUTE OF TECHNOLOGY

Pasadena

1937

CONTENTS

I. ABSTRACT

The shapes of the potassium resonance lines were obtained by a direct contour method. The pressures of the homogeneous absorbing vapor ranged from .001 to 20 mm Hg. The absorption coefficient was inversely proportional to the square of the distance from the line center. The half-breadths: varied linearly with the density of the absorbing atoms; were independent of the (relative) f-value of each line; yielded a Lorentz optical collision diameter of 200A. No asymmetries or shifts were detected. The experiment was made possible by the use of the new corrosion-resistant MgO windows.

II. INTRODUCTION

The subject matter of this thesis is concerned with the shapes of the potassium resonance lines ($\lambda\lambda$7664.94,7699.01) in absorption.

Light from a continuous source transmitted by an absorption cell containing a vapor of potassium is analyzed by a spectrograph. On the photographic plate of the spectrograph are recorded the familiar absorption lines, the density markings of which yield the transmission I/I_o* of the absorption cell as a function of distance along the plate, i.e., wavelength of light. The temperature and length of the absorbing column must be recorded for each spectrogram.

Consider a transverse section of the absorbing column of thickness dx, incident upon which is radiation of intensity I (a function of the wavelength). The decrease in intensity of the radiation in passing through the elementary layer is

$$-dI = \alpha I \, dx \, , \qquad (1)$$

where α, the factor of proportionality, is constant insofar as the explicit variables of the equation are concerned. Integration over the length x of the absorbing column yields directly

$$I/I_o = e^{-\alpha x} \, , \qquad (2)$$

*There is a considerable lack of uniformity of notation, especially as between German and American writers. In the present paper the notation used is for the most part chosen from that of the latter group.

where I is now the intensity of the radiation, of incident intensity I_o, transmitted by the absorption cell.

αx is known as the "absorption coefficient ". Equation (1) serves to define it. The verity of (2) rests upon the assumption of constancy of α in the integration. Such an assumption is inherent to our conception of the absorption process, at least as it exists in laboratory practice. Nevertheless, an incidental purpose of the present experiment is to test the dependence of the absorption coefficient upon the length of the absorbing column.

The absorption coefficient is a function of wavelength, and is determined as well by the conditions existing at the absorption cell. This experiment proposes to investigate this circumstance with (unique) emphasis upon the dependence of αx on N, the number of atoms per cubic centimeter, when N is "large".

A plot of an absorption line, the transmission I/I_o against wavelength*, is given in Fig. 1. Curve A represents the case of small absorption, curve B that where it is moderately large, i. e., practically complete at the center of the line.

*In theoretical developments, wave length enters either in circular or in frequency units. Because of ease of application, the wavelength measure $\delta\lambda = (\lambda - \lambda_o)$ where λ_o is the wavelength of the central maximum, will usually be used throughout.

The corresponding absorption coefficient as determined from (2), i.e., $\alpha x = \log_e I_o/I$, is plotted, αx against wavelength, in Fig. 2.

The range over which the transmission I/I_o of a line may be experimentally determined with any reliability is limited ($.9 > I/I_o > .1$, say). Accordingly, only a restricted portion of the course of the absorption coefficient is known ($.1 < \alpha x < 2.3$, say). (See E and F, Fig. 1 and 2).

The "half-breadth" (γ) of a line is defined as that wavelength interval over which $\alpha x \geq \frac{1}{2} (\alpha x)_{max}$, where $(\alpha x)_{max}$ is the maximum value attained by the absorption coefficient. For curves A and B, the half-breadths are indicated by the dotted lines C and D, respectively.

It is to be noted that in the case of curve B, the value of αx over the half-breadth is without the range of direct experimental measurement.

The area under the absorption coefficient curve determines the Einstein coefficient of induced absorption[1], for, according to Tolman[2],

$$B_{ij} = (c/h\lambda_o Nx) \int_{-\infty}^{+\infty} \alpha x \, d(\delta\lambda) \quad . \qquad (3)$$

This is related to the oscillator strength* (Ladenburg

*The oscillator strength, as properly defined, is an atomic constant. Nevertheless, some writers have designated as an f-value, a quantity which in fact (tacitly) depends upon the influence of neighboring atoms.

f-value) by[3]

$$f = (mhc/\pi e^2 \lambda_o) B_{ij} . \qquad (4)$$

Korff and Breit[4] have given a comprehensive review of the experimental determination of transition probabilities.

The half-breadth and area are quantities of considerable theoretical importance. They have a significance independent of the precise formulation of the absorption coefficient, other than that it satisfy (1). Unfortunately it is not possible to evaluate them individually with the present method, but rather simply their product, as will be seen.

III. THEORY

1. The Problem

The theoretical problem* is to formulate the dependence of the absorption coefficient upon the wavelength and the circumstance of the absorption cell. A great many effects are involved, all acting simultaneously. However, since the experimental attack may be modified such that but one or two of them is of measurable significance, a theoretical approach of the same pattern will serve the purpose.

The "natural breadth" of an absorption line is that finite breadth resulting from the absorption of light by a stationary isolated atom. Superimposed upon this is a broadening of the line due to the (thermal) motion of the absorbing atom, i. e., the Doppler effect. Finally, the course of the absorption coefficient is altered by the presence of other atoms in the vicinity of the active one.

Since theoretical developments usually lead to the so-called "dispersion equation", it will be given a moment's consideration here. It has the form,

$$\alpha x = \frac{\text{const}}{(\delta\lambda)^2 + \text{const}'} \quad ,$$

which is equivalent to

$$\alpha x = \frac{\varrho\gamma/2\pi}{(\delta\lambda)^2 + (\gamma/2)^2} \quad . \tag{5}$$

*A comprehensive summary of both theory and experiment has been given by Weisskopf[5], and by Margenau and Watson[6].

It may readily be seen that

$$\rho = \int_{-\infty}^{+\infty} \alpha x \, d(\delta\lambda) \quad , \tag{6}$$

i.e., ρ is the area under the absorption coefficient curve; that γ is the half-breadth; and that

$$(\alpha x)_{max} = 2\rho/\pi\gamma \quad , \tag{7}$$

(A plot of αx against $\delta\lambda$ is, in fact, that of Fig. 2).

The constants ρ and γ are determined by the conditions existing at the absorption cell, the interpretation depending upon the theory involved. However, in all cases considered herewith, the former constant is, simply,

$$\rho = \frac{\pi e^2 \lambda_o^2}{mc^2} Nfx \text{ (cm)} \quad , \tag{8}$$

and this value will hereafter be tacitly assumed. ((8) may be obtained in a roundabout way from (3), (4), (5), and (6), i.e., if theory yields the dispersion formula, and if (3) and (4) are correct, then (8) must always follow).

2. Natural Breadth

The first satisfactory approach to this question was based upon the electromagnetic theory of light[7]. The absorbing atom was considered as being a damped harmonic oscillator. The equation of motion, along the y-axis, of an oscillating particle of charge e and mass m, in the presence of a beam of light of amplitude E_o and frequency ν, propagated along the

the x-axis, is

$$m\ddot{y} = e\mathfrak{E}_o\, e^{2\pi i\nu t} - ay - b\dot{y} \,. \qquad (9)$$

The last two terms represent the forces of restitution and damping, respectively.

A particular integral is readily obtained. The current density due to this moving charge follows immediately. When Maxwell's equations, with the inclusion of the currents due to all oscillators, are solved in the usual manner, there results the dispersion equation (5). The half-breadth depends upon the damping factor b; the central wavelength upon a, i.e., the natural period of the oscillator. The theory gives no explicit evaluation to the constants a and b. Hence the value of the half-breadth and of the wavelength of the central maximum is not determined.

The latter, of course, is within the province of the quantum theory.

The former, however, was obtained with classical methods by Planck[8]. In (9) substitute for the damping force $-b\dot{y}$, the term, $-c\ddot{y}$, i.e., that damping force which results from the radiation of an accelerated charge. The method of solution remains unchanged. The value of c is given by the theory. Thus γ is determined, viz.,

$$\gamma = (4\pi e^2/3mc^2)\ (\text{cm}) = 1.17 \times 10^{-4}\ \text{A.}^* \qquad (10)$$

*A half-breadth of this magnitude is not directly measurable from an experimental contour, for want of a spectrograph of sufficient resolving power.

The expression "radiation damping" is frequently applied to the phenomena resulting in the natural breadth of a line.

A more elegant manner of solution is that of making a Fourier analysis of the electric moment of the vibrating particle. Consider first the general approach of this method[9]. The oscillator, of natural frequency ν_0, has an instantaneous frequency

$$\nu(\tau) = \nu_0 + \delta\nu(\tau) \quad , \tag{11}$$

where $\delta\nu(\tau)$ is that change of frequency resulting from external causes, if any. The electric moment of such an oscillator is

$$A(t)\, e^{2\pi i \int_0^t \nu(\tau)\, d\tau} \, ;$$

where A(t) is the amplitude, also a function of time. This expression, when developed in a Fourier integral, readily yields the absorption coefficient,

$$\alpha x = \text{const} \left| \int_{-\infty}^{+\infty} A(t)\, e^{2\pi i [\int_0^t \nu(\tau)\, d\tau - \nu' t]}\, dt \right|^2 \tag{12}$$

as a function of the spectral frequency ν'. That (12) takes all oscillators into consideration is implicit in the infinite limits of the integral, since the process of a single oscillator averaged over all time is the equivalent of the instantaneous average over all oscillators.

In the case of radiation damping $\delta\nu(\tau) = 0$, i.e., the frequency of the oscillator is unchanged. But the radiation is not coherent, for the oscillator is damped according to $A(t) = A_0\, e^{-\gamma t}$, where γ is precisely that half-breadth

given by (10). The analysis by use of (12) again yields the dispersion equation (5).

(10) indicates a half-breadth of line independent of the wavelength. Such is not, in fact, the case. Furthermore, the above electromagnetic theories fail to specify the value of the central wavelength; the classical quantum theory a finite region of absorption. The quantum mechanics throws new light upon the subject.

Weisskopf and Wigner[10], and Hoyt[11], have derived an expression formally identical to (5). The existence of a finite wavelength interval of a line is due simply to the fact that the energy levels of the atom are not perfectly sharp, by virtue of the indeterminacy principle. An expression is obtained for the half-breadth, one which depends upon the transition involved. However, for the case of the resonance lines of alkali metals (assuming the conventional f-value), the value of the half-breadth reduces to that given by (10).

3. Doppler Effect

Superimposed upon the distribution due to radiation damping, is that resulting from the (thermal) motion of the absorbing atoms. The Doppler effect widens the line, for the absorption coefficient at each wavelength is "spread out" in a Gaussian distribution[6]. The width of the latter depends upon the wavelength, and upon the temperature of the absorption cell, increasing with both. In the optical region, at temperatures employed in the laboratory, the Doppler broadening completely masks the true course of the central portion of an

absorption line of width otherwise determined by radiation damping. However, since the Doppler distribution is a relatively close one, the wings of a line are not appreciably affected.

Minkowski[12], after the Voight[13], has given a derivation in which the combined effects are quantitatively studied. He shows that for $|\delta\lambda| > 12\lambda_0 c_m/c$, where c_m is the most probable velocity of the absorbing atoms, an error of less than 1% is introduced by the neglect of the Doppler effect. In most practical cases, the line is of a breadth such that measurements can be (or must be) taken at a distance from the central maximum greater than that lower limit given above, and so the Doppler broadening may be ignored.

4. Pressure Broadening

Due to the presence of neighboring atoms, the normal process of the absorbing atom is disturbed, such that the absorption curve otherwise determined by radiation damping and the Doppler effect, is widened. This "pressure broadening" is, in the cases where it is being studied, usually of a relatively so much greater magnitude, that the other two effects may be ignored, (All three phenomena exist simultaneously to some degree, of course).

The various pressure effects may be loosely classified as follows: the Stark effect, wherein the presence of permanent charges (ions or poles) in the vicinity of the absorbing atom affects the normal process; collisions, result-

ing in an incoherence in the radiation because of interrupted absorption; resonance effect, a phenomena occuring from the presence of atoms similar to that performing absorption; the effect of "dispersion forces", i.e., the forces of a van der Waals type. It is to be emphasized that all of these effects are interrelated in the sense that they are more or less simply different interpretations of the same thing.

The Stark effect has been interpreted theoretically by Debye[14], and by Holtsmark[15], and studied experimentally by a number of others[16]. It is particularly successful in explaining the broadening of lines in gaseous discharges.* In the present experiment, there is no appreciable concentration of charged particles in the absorption cell; hence the Stark effect may be ignored.

The van der Waals forces exist whether or not the neighboring atoms are similar to that one performing the absorption. But in the former case, the effect is very small in comparison to that due to the resonance phenomena. Such is the situation in the present experiment, where, since dissimilar (foreign) gas particles are present only in negligible quantity, the effect of the resonance phenomena due to the presence of similar atoms completely overshadows

*The emission process and the absorption process are fundamentally identical.

that due to the van der Waals forces of similar (and dissimilar) atoms. The theory for the dispersion force phenomena is especially successful in explaining line shapes in the case where the foreign particles are in relative abundance[6]. This subject need not be considered here.

Before passing to the present day quantum mechanical approach to the problem of collision and resonance broadening, it will be well to consider a few of the older theories.

Classically, the resonance phenomena may be considered as arising in a coupling among the oscillating dipoles. The aggregate contains a great number of discrete frequencies distributed about the (unique) frequency of the individual dipoles. These are "spread out" by the Doppler effect, there resulting the broadened line. A theory based upon this coupling phenomena has been developed by Holtsmark[17].

Slater[18], using the classical quantum theory, obtained the dispersion formula presumably valid for high pressures. The half-breadth was not specified in terms of measurable quantities, however.

The foregoing theories are now only of historical interest. There is one, however, the Lorentz collision theory, that, by virtue of its sheer simplicity, has survived as giving an approximate description of the pressure broadening phenomena.

Lorentz[19] again assumes an oscillating dipole, the equation of motion of which is that given in (9) if the damping term be omitted. The dipole moment of the atom, starting from zero, increases with time until struck by a neighboring atom. This completely stops the absorption process, the energy of oscillation being converted into kinetic energy (collision of the second kind). The electric current to be substituted in Maxwell's equation is then determined from the electric moment averaged over all time intervals between collisions.

The solution again yields the dispersion equation, in which now the half-breadth is inversely proportional to the mean time interval between collisions. Then, from the kinetic theory,

$$\gamma = (\lambda_0^2 \rho^2 \bar{v} N/c) \quad (\text{cm}) \quad , \tag{13}$$

where ρ (not to be confused with the area under the absorption coefficient curve) is the "optical collision diameter", i.e., the average distance, between the centers of the colliding particles, at which the absorption process is interrupted, and N is the number of particles per cubic centimeter having a root-mean-square velocity $\bar{v}$ relative to the absorbing atom. The formula may be applied to the case of broadening by similar or by dissimilar atoms. From the kinetic theory,

$$\bar{v} = (8RT\ (M+M')/\pi MM')^{\frac{1}{2}} \ (\text{cm/sec}) \ , \tag{14}$$

where M and M' are the molecular weights of the absorbing

and disturbing atom, respectively*.

The same solution is obtained by making a Fourier analysis[6] of the electric moment of the absorbing atom, whose amplitude has a constant (sic) finite value over the time interval between collisions, but is nil otherwise, again averaged over all time intervals.

In either derivation, if radiation damping be included, the dispersion equation again obtains; the half-breadth γ is equal to the sum of the half-breadths of the two effects individually.

The more recent theories of pressure broadening will now be considered. Weisskopf[20] and Margenau and Watson[6], have derived the quantum mechanical analogy to (12) for the restricted case of A(t) = const. (11), in view of the relation $\nu = \epsilon/h$, is replaced by

$$\epsilon(\tau) = E_2 - E_1 + \delta\epsilon_2 - \delta\epsilon_1 , \qquad (15)$$

where E_2 and E_1 are the normal energies of the upper and lower quantum states, respectively, $\delta\epsilon_2$ and $\delta\epsilon_1$ the perturbations produced in these energies by the neighboring atoms.

The corresponding equation (12) for αx contains an interesting feature. Suppose that the perturbation energy is such that $\nu = \epsilon/h$, the frequency actually absorbed, lies

*Experimentally determined half-breadths indicate that (13) is incorrect when the kinetic theory value of ρ is used. It is customary rather to employ (13) to determine empirical values of ρ, these being somewhat larger than those of the kinetic theory. This result is not surprising, since con-

within a definite frequency interval. Because of the Fourier analysis (there is one involved in the quantum mechanical derivation as well), the absorption coefficient will in general have a finite value without this interval, i. e., at frequencies which the absorbing atom never had.

This circumstance is explained by Oldenberg[21] who considers the possibility of inelastic collisions (collisions of the first and second kind). The energy of the radiation is then determined not only by (15), but by the exchange of kinetic energy of the colliding pairs as well. In fact, it has been shown by Margenau[22] that the integrand of the expression for αx may be separated into two parts: the one the "statistical" distribution, i.e., that due to the perturbation energies; the other the "velocity" distribution, i. e., that due to the inelastic collisions; the two distributions being superimposed.

A complete rigorous determination of αx has not been made. An evaluation, good only for a restricted pressure range, has been given by Lenz[23]. To obtain a solution (approximately) valid for more general circumstances, it has been customary to consider the velocity distribution to the exclusion of the statistical one[24], or vice versa[25].

---

ceivably the absorption process may be disturbed without "collision" actually occuring. However, the Lorentz theory is not capable of predicting the values of ρ. A modified approach, which clears up this discrepancy, will be considered in the next section.

A simple illustration of the former case is the Lorentz collision process. A serious inconsistency is to be noted in this theory. Since presumably all the internal energy of the atom is, upon impact, transformed into kinetic energy (collision of the second kind), "quenching" of radiation would occur, a circumstance in general not verified experimentally.

A more satisfactory approach is given by Lenz[24] and by Kallman and London[24], with a modification by Kuhn[24]. The development is similar to that of Lorentz and yields the same dispersion equation. The distinction lies in the interpretation of ϱ, the "collision diameter". A perturbation process, in which the phase change of the radiation is of sufficient magnitude to result in incoherence, is in effect a collision. The total phase change φ of an encounter, in terms of the perturbation frequency $\delta\nu = (\delta\nu_2 - \delta\nu_1)$, is given by the relation

$$\varphi = \int 2\pi\,\delta\nu\,dt. \qquad (16)$$

Now the perturbation frequency (for resonance interactions) is[26]

$$\delta\nu = \pm(e^2 f/8\pi^2 m\nu_0)\,(1/R^3)\ , \qquad (17)$$

where R is the distance between the active and the perturbing atom, a function of time. Unfortunately, the perturbation energies due to each of several particles are not additive and the problem has not been solved. However, with the restriction of moderate pressures in the absorption cell,

and of observations at the wing of the line (which corresponds to close (single) encounters), (17) is approximately valid. Now ρ is specified as that distance of closest approach such that a unit phase change result from the encounter. (16) is thus its determination. The half-breadth, as obtained by substituting for ρ in (13), is

$$\gamma \cong (e^2\lambda_0^3/2\pi mc^2)\, Nf \text{ (cm)} . \qquad (18)$$

It is to be noted that (18) is independent of the velocity, i. e., an impact theory predicts a finite value of the half-breadth even when the (colliding?) particles are at rest. The apparent inconsistency has been clarified by Margenau and Watson[27]. They show, by the use of the statistical approach, that the dispersion formula is again obtained (with the restriction $|\delta\lambda| >> \gamma$), and that

$$\gamma \cong (e^2\lambda_0^3/6mc^2)\, Nf \text{ (cm)} , \qquad (19)$$

a value of the half-breadth which differs from that of (18) only by a factor of $2\pi/6$. They conclude that the concept of collisions, with an interaction distance ρ, is simply a different interpretation of a phenomena which might better be considered from the statistical viewpoint, in which case a dependence of ρ upon the velocity is not to be expected.

Thus, the theories for the case of broadening by similar atoms for the most part predict the (symmetrical) dispersion formula for the absorption coefficient, with varying interpretation as to the half-breadth. Although asymmetries and shifts may be expected[28], and have, in fact, been observ-

ed for helium in emission[29], the considerable difficulties in the way of experimental verification (as will be shown) render this phase of the subject of less interest.

In the case of broadening by foreign atoms, there exists a development similar to the entire preceding one[30], the principal difference being that strong asymmetries and shifts are predicted (and are observed).

IV. EXPERIMENTAL EVIDENCE

There are a number of experimental approaches to the subject. The most direct is that used here, i.e., that of obtaining of the actual line contour. Unfortunately, it is not always possible to measure the half-breadth directly, but rather, only the product $\rho\gamma$. In that case, in order to obtain γ, it is necessary either to assume a value of ρ (i.e., of f, since the other terms in (8) are known), or to determine it by some other method (that of magnetic rotation, say).

Though a great deal of experimental evidence has been amassed with respect to the shapes and constants of absorption lines, the bulk of it is concerned with the broadening caused by a foreign gas[30]. That case dealing with the line shapes resulting from disturbance by like atoms, however, has been successfully considered only for moderate pressures, for want of windows capable of withstanding attack of the hot vapors of the absorbing substance.

Minkowski[12], investigating the sodium resonance lines by a combination of the method of line contours and of magnetic rotation, verified the correctness of the theoretical contours, and of the half-breadth as determined by radiation damping (10), deviations setting in, however, at a pressure a little above 10^{-3} mm Hg. Korff[31], using the method of line contours, but assuming the value of ρ, arrived at conclusions

similar to those of Minkowski for both sodium and potassium. Weingeroff[32], by a procedure not unlike that of Minkowski, also obtained similar results. Again, Schütz[33] confirmed the work of Minkowski, but in addition noted a linear dependence of γ upon N in the pressure range 4×10^{-3} to 4×10^{-2} mm Hg, and upon N^2 at higher pressures.

Harrison and Slater[34], investigating the principal series of sodium by a line contour method, found that γ depended upon $N^{\frac{1}{2}}$ for a pressure range having an upper limit of about 10 mm Hg. A similar conclusion was reached by Trumpy[35] for both the sodium principal series, and for Hg 2537A, and by Waibel[36] for the principal series of ceasium. The results of Waibel are indecisive in that he investigated only a small pressure range (factor of about 3), and, furthermore, resorted to the doubtful technique of permitting of only ten minutes for his absorption cell to come to equilibrium from room temperature. The conclusions of Harrison and Slater, and of Trumpy, are probably vitiated by the presence of considerable pressures of a foreign gas (this last device was used to reduce the flow of the absorbing vapor to the cold windows).

Orthmann and Pringsheim[37], from an analysis of resonance radiation, determined a Lorentz collision diameter of ϱ=50A (Becker[38] investigating the HCl band spectrum, found a linear dependence upon N of the analogous half-breadth).

To sum the experimental evidence, the radiation

damping theory has been confirmed for pressures up to somewhat less than 10^{-2}mm Hg. Above this pressure, though the theoretical dispersion equation contour is verified, the half-breadth is variously determined as proportional to either $N^{\frac{1}{2}}$, N, or N^2. The latter results appear to be of doubtful validity either because of faulty technique, or of the smallness of the pressure range investigated. There does not seem to be any conclusive determination of the Lorentz collision diameter ρ, though it has been estimated in various ways[39].

In conclusion, therefore, it would appear that, for the case of a homogeneous absorbing vapor and for the pressure range above which the radiation damping theory is inadequate, the experimental evidence is not only meager, but contradictory.

It is the purpose of the present research to throw additional light upon this problem. A satisfactory conclusion is abetted by the use of especial corrosion-resistant windows, to be considered presently. As has been shown, theory leads for the most part to the dispersion equation (5) for the dependence of the absorption coefficient upon wavelength. This circumstance will be checked experimentally. If agreement is obtained, the constants will be determined, and compared to those predicted according to equations (8), (10), (13), (18), and (19).

V. EXPERIMENTAL PROCEDURE

1. Source

There are three requirements of the source: it must emit continuous radiation of approximately constant intensity over a wavelength region somewhat greater than that part of the spectrum appreciably absorbed by the lines; it must be of high intensity; it must be of radiating area and aperture of magnitude sufficient to satisfy the geometry of the optical system. A special tungsten lamp was built for this purpose. Specifications were determined from data in an article by Forsythe and Worthing[40] giving an exhaustive discussion of the properties of tungsten.

The lamp is illustrated in Fig. 3. The glass bulb (A) is approximately 13 cm in diameter. The filament (B) is supported with two nickel electrodes (C) by means of two small holes drilled through the ends of the latter. The electrodes are screwed into copper rods (D), which in turn are attached with Housekeeper seals (E) to a glass "plug" having a ground joint (F). The filament consists of a tungsten wire of approximately 1 mm diameter and 2.5 cm length. The element nickel was chosen as the material for the electrodes because it combines high melting point with good conductivity. The window (G) is a disk of glass held by wax to the end of the cylinder which projects from the bulb, at a distance from the filament purposely great, in order to

minimize the amount of vaporized tungsten deposited thereon.

Inasmuch as the filament is operated at a very high temperature, and, accordingly, has a limited life, it is important that it be possible to replace it quickly. The process involves letting air into the apparatus; removing the ground-glass joint; inserting a new filament; refitting the ground-glass joint, having first smeared it with a little stop-cock grease; and re-evacuating. The time required is about ten minutes.

The current to the filament is supplied by means of a step-down transformer. The core from a burned out 10 kw. transformer was rewound so as to provide for the reduction of the (110 volt) line voltage to 5 volts. The secondary consists of five strands of No. 8 cotton-covered copper wire wound in parallel. The transformer is capable of delivering over 100 amperes without excessive heating. The lamp operates at around 80 amperes. The current is regulated by means of a variable resistance in the primary circuit.

To avoid the necessity of continuously watching the lamp, in order to know the length of time the filament had burned, a timing device was installed. It consists of an ordinary 110-volt synchronous-motor-driven clock, current for which is supplied by means of a door-bell transformer which increases the voltage received across a small part of the primary circuit resistance to that required to run the

clock. When the current in the secondary circuit of the main transformer ceases due to the failure of the filament, the clock stops.

The life of the filament depends, of course, upon the temperature at which it is operated. The optimum temperature is such as to give a life of about two hours. Using 80 amperes, the temperature of the filament, as measured by means of an optical pyrometer, is then approximately 3400° K. This operating temperature is well above that of most commercial lamps. Two or three changes of the filament usually suffice to give the required exposure.

The dimensions of the filament are suitable for the projection of an image onto the slit of the spectrograph. The emitted radiation is of course continuous, and reasonably constant over the lines.

It is well known that the life of a tungsten lamp is greatly lengthened (approximately 20 times) by operating the filament in an atmosphere of a few millimeters of pressure of nitrogen. It was found, however, that commercial nitrogen was unsatisfactory for this purpose because of the considerable amount of impurity (oxygen) included in it.

A purifying apparatus: hot copper to remove the oxygen, a liquid air trap to remove vapors and a five-gallon bottle to act as a storage tank for the purified nitrogen, was connected to the apparatus. Preliminary tests

indicated that the life of the filament was, indeed, increased by the introduction of nitrogen into the lamp. Unfortunately, before the apparatus was put to practical use, the storage bottle exploded, - - and was never replaced.

As an alternative source, the carbon arc was investigated. It is of high intensity, but, unfortunately, the potassium resonance lines show up. They arise from reversal in the outer layers of the atmosphere of the arc, due to the pressure of potassium originating in the impure electrodes. Attempts to remove the potassium by chemical treatment of the electrodes were unsuccessful. However, the absorption lines were apparently eliminated by blowing a stream of air across the arc during its operation. But in view of this uncertainty, and the more troublesome operation, the carbon arc was discarded in favor of the tungsten lamp.

2. Furnace

The furnace consists of an absorbing column placed within a heating element located in a vacuum tight enclosure. A simplified sketch is given in Fig. 4.

The outer part of the furnace is a jacket consisting of two concentric steel cylinders (A) with welded seams. Water is circulated through this jacket by means of two orifices (B and C).

The heating element is a porcelain cylinder (D) on which is wound a double thickness of molybdenum wire, the

outer layer lacking windings at the central portion. By regulating the amount of current supplied to each layer, it was thought possible to compensate for the greater heat loss occuring at the ends of the heating element, thus insuring more uniform temperatures throughout. Three electrical connections are required. One is supplied by the enclosing jacket and the other two by electrodes (E and F). These last are insulated from the outer jacket by means of glass cylinders (G and H), the joints being sealed with wax. Each is cooled by a jet of air.

The absorption cell (I) rests within the porcelain cylinder. It is a copper tube of appropriate length from the inside of which has been cut a groove for the placement of the solid potassium. The temperature is determined by means of a thermocouple (J) which fits into a small hole in the top of the absorbing column. A steel-to-glass joint (K) serves as an exit for the thermocouple wires, and conveys as well to the evacuating pumps. The absorbing column is sealed at the ends by magnesium oxide windows (L and M) which latter are supported by the copper tubes (N and O). Heat insulated contact with the ends of outer jacket is obtained by means of soapstone cylinders (P and Q).

To obtain an absorbing column of short length (2 mm) the design of the tube was modified to that shown in Fig. 5. The potassium is held in a hollow screw (A), there being an

orifice (B) leading to the absorption chamber (C). This design was chosen so as to insure a sufficient area of contact for the thermocouple. As a suggestion for a very short absorbing column, there might be inserted an MgO window of appropriate thickness between the two end windows.

At either end of the outer jacket is fitted a steel "plug" (Fig. 4, R and S) having a passage for light, to the outer end of each of which is attached with sealing wax a glass window (T and U). The "plugs" are fastened by bolts, vacuum tightness being obtained by means of rubber gaskets (V and W). One of the "plugs" contains a sylphon (X) and is so arranged that, by turning the head (Y), a tube (Z) is made to advance such as to press the MgO windows against the ends of the absorbing column (I).

The system is evacuated by means of a two-stage mercury diffusion pump backed by a Hyvac pump. A pressure (as measured by a McLeod gauge) of less than 10^{-5} mm Hg can be obtained. The precise value of the pressure is immaterial so long as it is not so sufficiently great as to result in a pressure broadening of the absorption lines or in excessive heat conduction.

Current was supplied to the heating element by the direct current generators located in West Bridge Laboratory. Using the voltage regulation on the generators, together with

certain precautions, it was usually possible to maintain the temperature constant to within one degree over the time required to obtain an exposure. By thoroughly polishing and chromium plating the inner surfaces of the water jacket and the "plugs", the power consumption was reduced tremendously (from 2000 watts to 50 watts at 500° C). This device proved adequate to remedy the difficulty previously encountered with the softening of the wax joints. The electromotive force of the (chromel-alumel) thermocouple was measured with a potentiometer.

Since the temperature determines the density of the potassium atoms in the absorbing column, a factor entering into the theoretical formulation, its precise evaluation is of importance. The thermocouple yielded normal electromotive forces when calibrated from the freezing point of metals, but when it was used in the furnace for the determination of the temperature of the absorption cell, inconsistent results were obtained.

Accordingly, that thermocouple used for the final set of observations was calibrated "in situ", i. e., it was put in the furnace in the manner of normal use, and, in place of potassium in the absorption cell, bits of appropriate metals were substituted, the melting temperatures of which presumably yielding a true calibration of the thermocouple.

The metals used were tin, lead and zinc. A copper sheet was bent into the shape of a cylinder such as to fit snugly into the absorbing column. A strand of each metal was extended horizontally with ends attached to the cylindrical copper sheet, and also a bit of each was rested on the bottom of the copper sheet in the form of a miniature pole. The furnace was then slowly heated, a plot of the measured electromotive force of the thermocouple against time, together with the time of melting of the metals, yielding a temperature calibration of the thermocouple.

The two samples of each metal were used in order to increase the accuracy. Conceivably, the vertical piece might collapse at a temperature lower than, and the horizontal strand at a temperature higher than, the melting point; the former because of softening, the latter due to the formation of an oxide coating. It was found that both the horizontal and the vertical bits of the tin and of the lead collapsed at essentially the same (respective) temperature, but in the case of the zinc the vertical piece collapsed at a temperature far below the melting point.

The temperatures, as yielded by this calibration, were uniformly higher than those indicated by the conventional calibration. The correction was in fact practically linear with the difference between the temperature of the absorb-

ing column and room temperature, being about 12.4° per 100°. This result is not surprising in view of the geometry of the furnace. The junction of the thermocouple (which is of necessity covered, here with Insalute) assumes a temperature intermediate to that of the (hot) absorbing column and the (cold) extremeties of the thermocouple leads.

Since the furnace was maintained as nearly as possible in the same condition as that existing when the absorption spectrogram is made, this procedure would appear to be justified. The principal source of error arises from an uncertainty as to the reproducibility of contact of the end of the thermocouple housing with the absorbing column. This circumstance is inherent to the use of a vacuum furnace of the present design. It is to be noted that the power consumption of the furnace, which is a measure of the temperature of the absorption cell to the extent that the heat loss from radiation and conduction does not change with time, indicated that the conditions for the two cases were similar. Thus the temperatures determined by the thermocouple according to the above calibration, were used in the subsequent computation of N, the density of the potassium atoms in the absorbing column.

The windows employed in the absorption cell were made from MgO crystals. It is because of their unique

resistance to attack by hot metallic vapors that this experiment was possible. Other investigators, using glass or quartz, were restricted to low temperatures, or, if higher temperatures were attempted, they were forced to resort to doubtful technique.

Windows of considerable promise were discovered by Dr. Hughes. He ascertained that, of the many substances tested, certain gems, in particular the sapphire, showed a resistance to corrosion. He succeeded in making small artificial sapphires (from powdered aluminum oxide fused in an oxy-hydrogen flame). However, a more satisfactory source of supply was found. Artificial sapphires could be purchased, with dimensions to order, from a firm in New York known as the "Artificial Sapphire Products Company" ($20.00 for a pair of windows, each 1/2" in diameter and 3/16" thick). These windows showed resistance to attack from hot alkali vapors considerably superior to that of glass or quartz, and, in fact, they would probably have sufficed, with modified technique, for the completion of this experiment. Incidentally, the transmission of these windows in the ultravoilet is similar to that of quartz.

During the course of this experiment, while using the sapphire windows, Dr. Brice (in this laboratory) completed investigation of the properties of MgO. He found[41] that it was capable of resisting attack to very high temperatures. At

no time during which the MgO windows were subsequently used to obtain the potassium resonance lines spectrograms, did they show signs of attack by the hot vapor (temperatures up to 500° C).

MgO crystals are formed at the outer surface of large ingots occuring at one stage of a commercial process for the manufacture of a refractory material. They are considered a waste product and may be obtained at nominal cost. The crystals cleave and cut readily, but some difficulty is experienced in obtaining a good polish. One is also restricted as to size. In the present experiment windows of diameters of 1/2" or of 3/4", and of about 3/32" thickness were used.

3. Spectrograph

The spectrograph used was a 21-foot focal length concave grating in a Rowland mounting (located in Room #1, Bridge Laboratory). The grating has about 6000 lines per centimeter with a usable width of 12 cm. The length of the ruling is 5 cm. The resolving power of the grating in the first order according to the Raleigh criterion, is about 70,000. A slit width of 36 microns is of comparable resolving power. The corresponding figures, according to the Mack, Stehn, and Edlen criterion[42], are 65,000 and 41 microns, respectively. The dispersion in the first order is 2.64 A/mm. (For references to grating theory and practice, see bibliography[48]).

Prior to use, the spectrograph was tested and adjusted. The slit was cleaned by drawing between the slightly compressed jaws a strip of writing paper previously soaked in alcohol. The zero of the slit micrometer was ascertained from the reading at the setting at which no light was transmitted (visually) and checked by the width indicated by the dimensions of the diffraction pattern of transmitted light. The grating surface was cleaned with alcohol and precipitated chalk. The grating was tested optically for position, tilt, and tangency to the Rolland circle, and photographically, using an iron arc as source, for focus. The tilt of the slit relative to the rulings was determined photographically by observing the sharpness of the iron arc lines, and the symmetry of their ends for a small aperture before the plate. It was found that the spectrograph required little adjustment over considerable periods of time.

The grating should be completely (and uniformly) filled with light, and, if one is to avoid loss of intensity at the plate because of the astigmatism of the spectrograph, the length of slit illuminated must not be less than about one centimeter. An image of the source was brought to a focus within the absorbing column by a concavo-convex lens, and again at the slit of the spectrograph by a similar lens. It was possible simultaneously to fill the grating and to have

about an 1½ cm length of the image at the slit. The latter gave a sufficient portion of the plate, considered transversely, uniformly illuminated for the subsequent trace of the microphotometer. The introduction of a lens of 73 cm focal length just before the slit aided in the uniform illumination of the grating. The spectrograph was used in the first order, a red (Wratten F) filter being placed before the slit to cut out higher orders.

4. Photographic Photometry

Presumably the principal source of error lay in the uncertainties of the photographic photometry. Accordingly, considerable attention was given to this phase of the subject. (For references, see bibliography[49]).

A photographic plate is exposed to light the intensity of which varies over the surface of the plate. It is necessary to interpret the observed density in terms of the intensity of the incident radiation, i. e., calibrate the plate. The method chosen, in view of the limitations of the apparatus (time element, non-stigmatic spectrograph, etc.), was that of a step-weakener placed before the plate, the light transmitted by which being recorded on the plate simultaneously with that for the absorption lines. A comparison of the density markings for a line to those for the step-weakener yields the (relative) intensity of the light over the line if the transmission of the step-weakener is known. It is to be noted that no question of the constancy of the exposure of the plate enters into the problem since the two records are obtained simultaneously.

In view of the restricted wavelength region to be required, a step-weakener made from a photographic plate was considered adequate. A (slow lantern slide) plate was exposed to light such as to have thirteen "steps", each 1½ mm wide. The exposure required for a given density (transmission) of a given step could be estimated in advance. Care was taken to insure uniform density of each step (see below for development technique, etc.).

The transmission of the step-weakener was determined in three ways: by a densitometer, using a red (Wratten F) filter to eliminate the shorter wavelength of the light from the incandescent lamp source; by a double-monochrometer at assigned wave lengths; and photographically in the spectrograph. The procedure in the last method requires elaboration.

The two step-weakeners were placed before the spectrograph plate in the position of subsequent use. The aperture was restricted such that a number of successive exposures could be obtained on a single plate by moving the carriage (transversely). The plate was given an exposure, and the step-weakeners removed. Then a series of similar exposures (equal time and intensity) were made at each setting of the plate carriage, the corresponding intensity of the light actually arriving at the plate being determined by that transmission of the rotating sector placed before the slit. A sample calibration plate is reproduced in Fig. 6a.

A trace of each exposed strip along the direction of variation of wavelength was made with a microphotometer. The transmission of a given step was immediately determinable from its deflection by interpolation between the deflection of those strips whose exposures were modified (in known amounts) by the rotating sector, at the wavelength corresponding to the step. This last is important since the sensitivity of the plate varies considerably with the wavelength.

By using a wide slit (500 microns), and thus short exposure time (10 minutes) and low intensity of the lamp (70 amp.), it was thought possible to attain sufficient constancy of the intensity of the source. The spectrograph plate used (IR) was hypersensitized with triethanolamine which gives a very uniform increased sensitivity, and carefully developed.

Until recently considerable uncertainty existed as to the ability of a photographic plate to "integrate" a discontinuous exposure such as that resulting from the presence of a rotating sector in the light path (the "intermittency effect"). However, it has now been shown[43] that an intermittent exposure of sufficient frequency is equivalent to the corresponding continuous one. For the wavelength under consideration a frequency greater than about 1000 per minute is satisfactory.

In the present case the rotating sectors were mounted directly upon the spindle of a motor making about 1700 revolutions per minute. They consisted of circular (cardboard) disks with apertures in the form of sectors. The transmission of the rotating disk is then simply the ratio of the central

angle of the sector to 2π. Seven sectors were used with transmissions down to 1/16th.

A tabulation of the measured transmission of a step-weakener is given in Table I. No significant variation was found between the two step-weakeners used.

TABLE I

Step-Weakener Transmission in Percentum

Step	1	2	3	4	5	6	7	8	9	10	11	12	13
Densitometer	87	68	61	55	47	40	29	22	15	10	5	2	1
Monochrometer	89	72	64	58	49	42	31	23	15	9	5	2	1
Photographic	98	90	85	80	73	65	55	45	35	25	17	12	10

Furthermore, the transmission did not vary appreciably with the wavelength, over the range required. It is to be noted that the transmissions are greater for the monochrometer calibration than for that of the densitometer, and are still larger for the photographic calibration. This is explained by the fact that a different kind of transmission is measured in each case.

It is known that light transmitted by a photographic plate does not show simply partial absorption, but scattering as well[44]. The "transmission" depends then upon the effective solid angle at the plate over which the transmitted light is measured (and upon the density, and type of emulsion). The limiting transmissions are known as diffuse and specular, the former corresponding to a solid angle of 2π, the latter to that small solid angle through which the

bulk of the light passes.

In practice, the transmission measured is usually intermediate to that of the limiting values. An optical projection system, such as was used for the densitometer and the monochrometer calibration, results nearly in the specular type, since scattered light is lost; the step-weakener just before the plate nearly in the diffuse, since the light reaching the spectrograph plate at a given point behind a step comes from all parts of that step and from adjacent steps as well.

Numerical computation indicates that the higher values of the photographically determined transmissions may be explained by these considerations (the transmissions given by the densitometer calibration are not strictly comparable, since the light used is not monochromatic). Accordingly, these step-weakener transmissions were used. Unfortunately, this increases the uncertainty of the final results, inasmuch as reliance is placed an additional time upon photographic photometry. Furthermore, an inconsistency is to be noted. The relative intensity, as determined by the use of a step-weakener before the plate, is independent of the constancy of the intensity of the source; whereas the method of calibration here used requires the assumption of constancy during the calibration exposures. However, in the latter case the conditions could be more readily controlled.

The step-weakeners were mounted just before the

spectrograph plate (separation 1½ mm), one on either side of the pair of absorption lines, with the steps parallel to the lines (the spectrograph being astigmatic, it is not permissible to have them perpendicular to the lines).

The plates used were Eastman type IR. These are the fastest ones available in the wave length region corresponding to the potassium resonance lines (other plates considered were type IK and type IN). Prior to exposure the plate was hypersensitized with ammonium hydroxide. This has the effect of greatly increasing the sensitivity. However, some difficulty was experienced in obtaining uniform sensitization. The procedure finally adopted was to bathe the plate for 1½ minutes in a 4% solution of 15N ammonium hydroxide, thereafter rinsing it one or two seconds in distilled water, shaking, and drying rapidly before a fan in a dust-proof enclosure. The water rinse apparently avoids the blotches that would otherwise result from the irregular drying of the plate. No satisfactory results could be obtained by the removal of the droplets of hypersensitizer with an airblast, or wiping with a sponge, say.

An increase in the concentration of the hypersensitizer or of the bathing time results in excessive fog. Though it is recommended that the hypersensitizing solution be chilled before use in order to minimize fogging, it was found that this precaution was not necessary in the present case (usual temperature of the bath about 20°C). Reasonably uniform plates were thus obtained with an increased speed of

four to five times. However, tests showed some deviation from the theoretical Hurter and Driffield curves, failure of a single intersection point of the straight line portion, and decreased latitude.

More uniform hypersensitization could be obtained by bathing the plate in a ½% solution of triethanolamine with a similar technique, but there resulted only about one-half the sensitivity of that of a plate bathed in ammonium hydroxide.

The plate was used immediately after drying to avoid the fogging which results from prolonged standing. The exposure was restricted to the central portions of the plate to eliminate "edge" effects. Exposures were regulated so as to have the major portion of the absorption line fall upon the lower part of the straight line portion of the characteristic curve. Excessive exposure, aside from being uneconomical, overtaxes the measuring capacity of the microphotometer.

The developer used was Eastman formula D-19, 25% solution. A 5-minute development gives approximately unit gamma (without excessive fog). This is desirable because of the increased accuracy of measurement which results when the opacity of a plate varies linearly with the exposure. To insure even development the plate was continuously rubbed with a camel's hair brush. The brush was motivated by a reciprocating device driven by an electric motor. The stroke was equal to the length of the plate

used. The period was a little over a second. It was thought that this brushing insured considerable uniformity over the plate; for example, the Eberhard effect was practically eliminated. Brushing caused little change in gamma. The plate was fixed in Eastman formula F-1 in the usual manner, thoroughly washed in running water, rinsed off with distilled water, and set to dry slowly, emulsion side up, in a ventilated dust-proof enclosure.

5. Operating Technique

The absorption cell, together with the MgO windows and end tubes, is placed within the porcelain heating element; the thermocouple is lowered into contact with the cell; and the end pieces of the furnace are attached. The system is evacuated and then heated to a temperature somewhat above the maximum to be attained in subsequently obtaining the spectrograms. The purpose of this is to free the absorbing column from occluded gases which otherwise might cause a pressure broadening of the absorption lines. The furnace is then cooled off and opened up. Potassium cut under xylene is packed into a tiny five-sided sheet-steel "box" which is placed open face downwards in the groove at the center of the absorption cell. The furnace is quickly closed up and evacuated. The potassium is cut under xylene to reduce oxidization, the vapor pressure of the xylene being sufficiently high so as to evaporate away before the absorbing column is sealed off.

As soon as a good vacuum is obtained, the furnace is heated to a temperature slightly above the melting point of the potassium and permitted to stand for several hours. This, presumably, releases the bulk of the gases contained in the potassium. A preferable technique would involve pre-distillation of the potassium.

The absorption cell is then sealed off by rotating the head on the sylphon, such that the MgO windows are pressed against the end of the tube. A small raised ring at either end of the absorbing column serves as a gasket, the copper being sufficiently soft to compress readily. A good seal is usually obtained.

The furnace is then raised to an appropriate temperature and a spectrogram of the light transmitted by the absorbing column is made. The furnace is then raised to the next temperature, and another spectrogram made, and so on. Exposure times varied from 2 to 20 hours. The shorter exposures were used for the higher temperatures, where, since the lines are wider, the opening up of the spectrograph slit is permissible.

Under favorable circumstances a picture could be obtained during the daytime, the furnace coming to equilibrium at the next temperature over night. Since, in any case, it requires several weeks to obtain a set of pictures, with the apparatus in continuous operation, time was of the essence if success was to be obtained.

At higher temperatures the MgO windows become coated with (droplets of) potassium. This had the effect of increasing the required exposure time because of the reduced transmission of the windows. Furthermore, it indicated that the windows were the coldest part of the absorption cell, a fact otherwise suspected. In equilibrum, the pressure of the vapor is determined by the temperature of the coldest part of the cell. It was thought, however, that the measured temperatures were not greatly in error in view of the superior heat conducting qualities of the copper absorbing column and the smallness of the solid angle through which heat might be permanently lost by radiation.

In the case of the shortest tube used the potassium escaped at the higher temperatures, i. e., the seal was imperfect. This means that complete thermodynamical equilibrium did not exist, but the error introduced was probably small.

VI. REDUCTION OF OBSERVATIONS

1. Microphotometer

A Krüss microphotometer was used to obtain a trace of the plates (at present located in Room #14-a Astrophysics Building). A description of the microphotometer is as follows.

Briefly, light from a tungsten lamp transmitted through an optical slit at the (spectrograph) plate to be measured falls upon a photo-electric cell. The cell activates the string of an electrometer, a magnified image of which is recorded on another (the microphotometer) photographic plate. Simultaneous motion of the two plates, with given relative speeds, produces a continuous trace of the string image on the microphotometer plate; the ordinate of which is determined by the deflection of the string, i. e., is a measure of the transmission of the spectrograph plate; and the abscissa of which is proportional to distance along the spectrograph plate, i. e., wavelength of light.

The light from a slit before the lamp is focused on the spectrograph plate, then on a slit before the photo-electric cell, and finally upon the sensitive element of the cell. The effective slit dimension is determined by the (reduced) size of the image of the slit located before the cell, at the plate. The (fixed) slits supplied with the apparatus are such as to give effective width of 10 microns up, and length of the order of 1 mm.

The illuminated cell is connected electrically with a second photo-electric cell, which latter acts as a controlled leak, the purpose of which being to minimize the effect of variation of the intensity of the source. The sensitivity of the system, i.e., the magnitude of the deflection of the string for a given effective slit area, is determined by the amount of light from the source that falls upon the cell that acts as a controlled leak, and by the tension of the string in the electrometer.

The size of the microphotometer plate is 9 x 24 cm, with a usable area of 8 x 23 cm. A guide line is optically recorded on the plate to serve as reference for the ordinate.

The carriage of the spectrograph plate is connected to that of the microphotometer plate by a system of levers and cables, such that the motion of the latter carriage results in a prescribed motion of the former. The permissible ratios are 1:1, 2:1, 6:1, and 40:1, i. e., distances along the spectrograph plate are magnified on the microphotometer plate by these amounts. The carriage system is motor-driven and completely automatic.

It is to be observed that if the apparatus be operated at high sensitivity some error is introduced by the lag of the string of the electrometer, which offsets the advantage of the increased deflection. The magnitude of the lag may be reduced by increasing the area of the effective slit, where permissible, and by retarding the motion of the carriage.

However, this latter device must be used with caution, since error will be introduced by the greater effective drift of the zero point of the string. For the running time of 15 to 20 minutes, correction for the drift was not necessary, and, furthermore, in view of the absence of sudden large changes in the density of the photographic plates measured, the error introduced by the lag was negligible if moderate sensitivity was used.

The carriage ratios were tested as follows: a trace of a 1 mm length interferometer scale was made on the microphotometer plate. The accuracy of the divisions of the scale was previously ascertained with a comparator. A comparison of the separations on the plate of the deflections corresponding to where the slit passed over a division of the scale, to the actual separations of the divisions, yielded immediately the value of the magnification. The 40:1 magnification required an average correction such as to read rather, 39.8:1. No correction was necessary for the other magnifications.

2. Comparator

Inasmuch as it is required to read simultaneously the ordinate and the abscissa of the microphotometer trace, it is necessary to use a comparator, with two-dimensional motion. The one used reads to .001 mm in the horizontal motion and .01 mm in the vertical motion, with a range

of 20 cm and 2½ cm respectively. The accuracy is then more than ample and the range is adequate.

It is to be observed that the tedious comparator reductions could be eliminated by the use of a microphotometer that automatically gives an enlarged record on graph paper.

3. Graphical Interpretation

A large number of operations is involved in interpreting the density markings of the spectrograph plate in terms of the constants of the absorption lines. It is, therefore, important that one have a carefully thought out system if one is to avoid errors and is to reduce labor. The following method was used for most lines. Certain remarks will be qualified presently.

A trace by the microphotometer of that portion of the plate which includes the two step-weakener images and the two absorption lines, magnified 2:1, covers about 15 cm. This leaves about 4 cm each for a highly magnified trace of the lines in a 40:1 ratio, say, the entire record being thus obtained on a single microphotometer plate. (For a reproduction of a trace see Fig. 6b. The highly magnified lines are not shown). The comparator can accommodate the plate lengthwise in two settings, once for the enlarged trace of the lines and once for the trace of the step-weakeners. The relatively few readings of the latter can be easily translated so as to have the same origin of ordinate as the lines. It is

usually possible to align the plate in the comparator sufficiently well so as to avoid necessity for correction.

The sensitivity of the microphotometer was regulated such that the deflection over an absorption line covered about 2½ cm. Thus one can get all ordinate readings with a single setting of the plate, the overrun of the vertical motion of the comparator carriage permitting the determination of the ordinate of the zero deflection (for drift check), and of a step or two below the bottom of the lines, if any. This reduction in the possible amount of the microphotometer deflection offsets the lag, but, in any case, the accuracy of the comparator, and the ability to set the cross-hairs of the telescope on the trace, are never taxed.

The trace of a step is irregular, but one may readily set at an average value, as related to the horizontal cross-hair of the telescope, with sufficient accuracy (.1 mm). This is consistent with the manner of setting on a step used in the calibration of the step-weakener. The value of the abscissa of a step is unimportant except insofar as it enters into the correction for the varying sensitivity of the plate with wavelength, to be considered presently.

For the determination of the coordinates of the lines, the vertical motion was set at 1 mm intervals, thus giving about 25 points for each wing, the horizontal setting being read simultaneously, to the nearest .1 mm usually sufficing

(this is dependent upon the width of the trace of the line, i. e., inherent width of the line times magnification).

The reason for using fixed interval settings for the vertical motion instead of the horizontal is two-fold. First, the scale of the horizontal motion is easier to read; secondly, $\delta\lambda$ may thus be determined as one-half the difference of the abscissa of the two wings for the same ordinate. This "averaging" procedure was used inasmuch as it not only avoids the necessity of ~~the~~ determining absolute wave length each time, but it also halves the work of the subsequent reduction. The procedure has been justified by the inability to detect any asymmetry or shift of the lines (except as will be seen).

The averaged wing is then plotted on (roll) millimeter graph paper (A, Fig. 7). The height of the graph paper being 50 cm. a magnification of 20:1 is provided for the $2\frac{1}{2}$ cm range of the ordinate of the trace. The full breadth of the line, in millimeters, as given by the difference of the abscissa of the trace for each ordinate, is multiplied by d/2m, where d is the dispersion of the spectrograph (2.64 A/mm), and m is the magnification of the microphotometer, the factor one-half being introduced to give half the total width. The resulting numerical figure ($\delta\lambda$ in A) is plotted as abscissa, the scale being adjusted such that the usable portion of the line covers about 50 cm on the graph paper. On the same sheet is plotted the step-weakener readings, the ordinate being the same as that of the lines, the abscissa being the (known)

trans

transmission (I/I_o) of the steps.

The curve for the step-weakener (B, Fig. 7) represents the idealized case of a plate that is uniformly sensitive with wavelength, the (normally distinct) plot for each step-weakener coinciding. Unfortunately, the plates used showed a marked decrease in sensitivity to the shorter wavelength. A single rigorous correction for this deficiency is not possible since for each plate there is a variation in exposure, gamma (development time), inherent sensitivity, and sensitivity of the micro-photometer. However, the use of two step-weakeners restricts the correct step-weakener trace to a position intermediate to the two observed.

Accordingly, the curve to be used (one for each line) is arrived at by considering the sensitivity of the plate at each step with respect to that at the line under consideration, the general variation of the sensitivity of the plate having been determined by a trace of the continuous background (from a plate exposed without step-weakener or absorbing column in position). It is to be noted that an averaging of the two halves of a line is not permissible for wide lines, inasmuch as the varying sensitivity of the plate over a line becomes a real factor.

By means of the corrected step-weakener curve, the ordinate of the line plot may be changed from electrometer deflection to true transmission I/I_o, the abscissa remaining

unaltered in Angstrom units. This is done most simply graphically, i.e., at convenient intervals of the abscissa of the (absorption line) microphotometer curve, the transmission is determined from the abscissa of the step-weakener curve of that point of corresponding ordinate (as indicated by the straight dotted lines, Fig. 7). The absorption line curve is thus turned through a right angle (and reflected). It is not essential that the second curve (C, Fig. 7) actually be drawn out, but it was usually so done as a check on the nature of the line. In any case, one may tabulate the transmissions (I/I_o) corresponding to each wavelength $(\delta\lambda)$ of the line wing.

Let us consider the functional relation

$$I/I_o = e^{-\alpha x} = e^{-[(C \log_e 10)/[(\delta\lambda)^2 + CC']]}, \qquad (20)$$

a form for the absorption coefficient more suitable than (6) for graphical interpretation. Solving for $(\delta\lambda)^2$,

$$(\delta\lambda)^2 = C\,(1/\log_{10} I_o/I + C'). \qquad (21)$$

Then a plot with $(\delta\lambda)^2$ as ordinate against $1/\log_{10} I_o/I$ as abscissa, is a straight line with slope C and intercept C' .

A plot of the experimental values of $(\delta\lambda)^2$ and $1/\log_{10} I_o/I$ in fact shows such a linear relation (D, Fig. 7). Of course the experimental plots show deviations from linearity, especially at the extreme portions. At the bottom of the absorption line the measured transmission is too large (Doppler effect, scattered light, etc.) and for both this portion and the extreme

wings, deviation occurs because of the inherent difficulty of accurate measurement. However, the plot corresponding to the usable part of the absorption lines was approximately straight.

In practice it was found that C' was sensibly nil*. This means that nearly complete absorption was occuring at the bottom of the line, since C' is inversely proportional to $(\alpha x)_{max}$. Accordingly, a straight line passing through the origin was fitted to the empirical plot, and its slope recorded.

The problem is equivalent to that of the determination of the best value of C from a set of pairs of values of $\delta\lambda$ and I/I_o, where now $C = (\delta\lambda)^2 \log_{10} I_o/I$. Both methods yielded similar results. The former had the advantage of ease of interpretation and of detection of systematic deviations. It is to be emphasized that great accuracy in the determination of C was not possible. (A similar method of graphical interpretation has been used by Harrison[34]).

In addition to the foregoing reduction, the "width" of each line was measured by observing it on the spectrograph plate with the aid of the comparator. The assumed "edge" of the line corresponds to some (unknown) value of the transmission I/I_o (.9, say). The square of half of the measured

---

* For a discussion of this and some related subjects see Appendix I.

"width" is thus proportional to C. This method fails for narrow lines, which, being incompletely resolved, appear to be too "wide", and for wide lines, in which case it becomes increasingly difficult to determine the true "edge". Since no great reliance may be placed upon the results, they serve only as a check on the (relative) values of C. The principal recommendation of this device is that it eliminates all errors associated with the step-weakener, the microphotometer, and the reduction of observations.

Of the many sources of error of the photometry, the following, which permit of some quantitative measurement, bear consideration: the finite resolving power of the microphotometer; the finite resolving power of the photographic plate; the finite resolving power of the spectrograph; the variation of the intensity of the source with wave length.

As to the microphotometer, the lag and drift of the electrometer string has already been considered. Failure of precise linearity of deflection with transmission was not a factor since calibration was done by means of the step-weakeners. The effective slit width used for the narrower lines was 10 microns, which corresponds to a theoretical resolving power greater than that of the plate or of the spectrograph.

A convenient correction formula for a finite slit width of this type is given by Slater[45]. He shows that the observed value of the ordinate $f(\delta\lambda)$ at a point of abscissa

$\delta\lambda$ (on the microphotometer trace) has a correction $- 1/6\left[\frac{1}{2}(\delta\lambda+a/2) + f(\delta\lambda-a/2) - 2f(\delta\lambda)\right]$, where a is the effective slit width. Graphically, one substracts (algebraically) one-third of the distance, along the ordinate, from the point under consideration to a chord joining the two points of the curve lying on either side at a distance along the abscissa equivalent to one-half of the slit width. This correction was applied to the narrower lines; it resulted in no great change in the contour.

For wider lines a microphotometer slit width of 20 microns was used. The length of the slit (of the order of 1 mm) was adequate to avoid the error that might be caused by the fact that the density of a photographic plate arises from the presence of discrete opaque particles in the emulsion. Care was taken to align the spectrograph plate in the microphotometer carriage such that the motion was precisely along the direction of the changing wavelength, to avoid error that would otherwise arise inasmuch as the density perpendicular to this direction is not uniform (astigmatism, etc.). The slit was then automatically parallel to the lines.

The resolving power of the photographic plate, loosely speaking, is about three times that of the grating. This was of necessity considered adequate, for a plate of greater resolving power would lack the required speed.

As to the spectrograph, the theoretical resolving power of the grating has already been discussed. The slit width used for the narrower lines was 15 or 20 microns, corresponding to a resolving power about double that of the grating. For wider lines, slit widths up to 100 microns were used.

The foregoing sources of error have the common feature that they tend to broaden a line, and they are of relatively greater significance for narrower lines. A device due to Landenburg and Reiche[46], and tested experimentally by Minkowski[12], corrects for these failures of resolving power treated as a whole. The principle used is that, though due to these effects a line is broadened, the area of the line $\int_{-\infty}^{+\infty} (1 - I/I_0)\, d(\delta\lambda)$, remains constant, and this area is equal to $(4\pi C \log_e 10)^{\frac{1}{2}}$ (see Appendix II). This method was used for the narrower lines, apparently with consistent results. For lines of even moderate width, however, the device fails since the position of the wings of the line is not accurately known. The use of a planimeter to determine the area (and hence C) is indeed simple.

The variation of intensity of the source with wavelength, as determined from computations which treat it as a black body, is negligible over the range used, especially in view of the uncertainty due to the varying sensitivity of the plate.

In addition to the above, the Doppler effect presents a possible source of error. But for the narrower lines, simply the area was determined; for the wider ones, measurements were always at points without the region of influence of the Doppler effect. (If $|\delta\lambda| > .14$ A, then for $T = 500^{\circ}$ K, the error is less than 1%). Hence it could be ignored.

The very wide absorption line presents special problems. The sensitivity of the plate now varies considerably over the line*. Then, greater uncertainty is introduced with respect to the varying sensitivity of the plate inasmuch as it is necessary to increase the separation of the two step-weakeners. Furthermore, the wings of the line appreciably absorb light in the wavelength regions at which the step-weakeners are located. Finally, the two absorption lines begin to show overlapping. From a knowledge of the course of the trace for the four possible cases involving the absorption lines and the step-weakeners, i.e., when both, neither, or either, modify the continuous background, it is possible to correct for all but the last effect. It is to be emphasized that great accuracy is not attainable. Note also that most theories are based upon the assumption of $|\delta\lambda| \ll \lambda_0$.

* Obviously it is no longer permissible to average the wings of a line.

The question of the overlapping of lines merits detailed consideration. In Appendix III it is shown that for the majority of cases, the error introduced into the measurements because of overlapping is less than 10%. In no case is it greater than 200%.

The foregoing considerations are concerned simply with the widths of symmetrical lines. Two further effects bear investigation, viz., the question of asymmetries, and of shifts of the absorption maximum. Absolute wavelengths were determined by means of a spectrum of the iron arc photographed on the spectrograph plate. The conclusion was reached that, within the wide limit of uncertainty of measurement, no shift or asymmetries occurred. But by the very nature of the observations, it would not have been possible to detect them unless they were very large. The reason for this lies in the inherent difficulty of determining an asymmetry, or a shift of $(\alpha x)_{max}$, from a knowledge of the value of αx at a portion of the wings, particularly in view of the fact that any conclusions as to the one effect would modify those with respect to the other. (The problem is not unlike that of determining absolute transition probabilities).

A slight confusion was introduced into the observations because of the presence of foreign spectra, namely, the rubidium resonance lines, oxygen bands, and a structure in the long wavelength wing of the overlapping lines at high pressures[47].

For a reproduction of several spectrograms, see Fig. 6c. They correspond, in the order of increasing width, to pressures of .0041, .16, 1.5, and 20mm Hg, respectively. The first is unresolved, the third begins to show overlapping, the last is completely overlapped. (Note the structure in the wings).

4. Auxiliary Variables

In addition to determining the constant C, two other quantities must be measured, the length of the absorbing column and the temperature.

The measurement of the tube-length presents no difficulty except for the very short tubes. In this case, since the MgO windows do not collapse the two copper seals quite uniformly, i.e., the inner faces of the windows are not strictly parallel, only an average value can be taken (measured with a micrometer). The tube-lengths used varied from .213 cm to 15.3 cm, a factor of 72. (A short tube length decreases the width of an otherwise wide line, and conversely).

The temperature of a saturated vapor uniquely determines its density. From the International Critical Tables

$$\log_{10} p = \frac{-52.23 \times 84.9}{T} + 7.183$$

where p is the pressure of the vapor in millimeters of vapor in millimeters of mercury, and T the absolute temperature.

Unfortunately, the lower limit of the experimental verification of this formula is at 260°C, corresponding to a pressure of about .09 mm. For want of additional information the above formula was used over the entire temperature range. Then N, the number of atoms per cubic centimeter is (assuming the Boyle, Gay-Lussac Law),

$$N = 9.70 \times 10^{18} (p/T).$$

The temperature range for the final set of observations extended from 444°K to 755°K, corresponding to pressures of from 1.6×10^{-3} to 20.4 mm Hg, a factor of 7400 in N.

In the subsequent computations, the conventional f-values were assumed, viz., $f_1 = 2/3$, $f_2 = 1/3$ (λλ7665,7699, respectively).

VII. RESULTS

1. Relative Values

In Table II are summarized the results derived by the foregoing considerations. Tabulated by column, are the absolute temperature of the absorption cell, the pressure in mm Hg, and the number of potassium atoms per cubic centimeter. The next two columns give the observed values of the constant of the dispersion formula (20) for the short and long wavelength component, in that order. In the case of Plate 43, the lines completely overlapped, and, accordingly, but the sum ($C_1 + C_2$) was measurable. (The lines practically fill the length of the plateholder). Next is shown the ratio $C_1 : C_2$, and the ratio of C_1 and C_2 to $N^2 f_1 x$ and $N^2 f_2 x$, respectively. The appropriate tube length x for each set of plates is as indicated.

The theoretical value of C is, from (5) and (20),

$$C = \rho\gamma/(2\pi \log_e 10) \ . \qquad (22)$$

Now, in all cases, from (8),

$$\rho = (\pi e^2 \lambda_o^2/mc^2)\ Nfx \quad (cm) \ . \qquad (23)$$

For radiation damping, from (10)

$$\gamma = (4\pi e^2/3mc^2) \quad (cm) \ . \qquad (24)$$

For Lorentz collision broadening, from (13),

$$\gamma = (\lambda_o^2 \rho^2 \bar{v}/c)\ N \ (cm) \ . \qquad (25)$$

For the modified Lorentz theory, from (18),

$$\gamma = (e^2 \lambda_o^3/2\pi mc^2)\ Nf \quad (cm), \qquad (26)$$

TABLE II

Pl. No.	T(°K)	p(mm)	N	$C_1(cm^2)$	$C_2(cm^2)$	$\frac{C_1}{C_2}$	$\frac{C_1}{N^2 f_1 x}$ x10^{47}	$\frac{C_2}{N^2 f_2 x}$ x10^{47}
				Tube Length .240 cm				
33	463	4.08×10^{-3}	8.55×10^{13}	5.13×10^{-20}	2.63×10^{-20}	1.95	4.38	4.49
34	498	1.91×10^{-2}	3.72×10^{14}	4.48×10^{-19}	2.20×10^{-19}	2.02	2.03	1.98
35	518	4.17	7.81	2.16×10^{-18}	9.10	2.37	2.21	1.86
36	555	1.59×10^{-1}	2.78×10^{15}	1.88×10^{-17}	9.41×10^{-18}	2.00	1.52	1.57
37	593	5.13	8.38	2.45×10^{-16}	9.49×10^{-17}	2.58	2.19	1.69
38	633	1.51×10^{0}	2.31×10^{16}	1.45×10^{-15}	8.60×10^{-16}	1.69	1.70	2.02
					Average		2.29	
				Tube Length .213 cm				
40	584	3.98×10^{-1}	6.61×10^{15}	1.81×10^{-16}	8.90×10^{-17}	2.03	2.92	2.87
41	664	3.16×10^{0}	4.62×10^{16}	7.93×10^{-15}	4.17×10^{-15}	1.90	2.61	2.75
42	696	6.46	9.00	2.50×10^{-14}	1.00×10^{-14}	2.50	2.17	1.74
43	755	2.04×10^{1}	2.62×10^{17}	$(C_1+C_2) = 2.60\times10^{-13}$			1.78	
					Average		2.33	
				Tube Length 15.3 cm				
44	444	1.62×10^{-3}	3.54×10^{13}	1.72×10^{-19}	1.02×10^{-19}	1.69	1.34	1.60
45	461	3.62	7.62	8.52	4.77	1.79	1.44	1.61
46	481	9.12	1.84×10^{14}	7.75×10^{-18}	3.43×10^{-18}	2.26	2.22	1.98
47	516	3.89×10^{-2}	7.50	1.04×10^{-16}	5.31×10^{-17}	1.96	1.81	1.85
48	545	1.12×10^{-1}	1.99×10^{15}	1.27×10^{-15}	5.80×10^{-16}	2.19	3.14	2.87
					Average		1.99	
	560				GRAND AVERAGE	2.07	2.20	

For the Margenau and Watson derivation, from (19),

$$\gamma = (e^2\lambda_o^3/6mc^2)\ Nf\ (cm), \qquad (27)$$

Now, as subsequent examination of the data will show, the pressures used are higher than those at which radiation damping is of significance, and so (24) may be ignored. Thus, using (22) and (23), in conjunction with either: (25); or (26); or (27); then, respectively:

$$C = (e^2\lambda_o^4\rho^2\bar{v}/2mc^3\log_e 10)\ N^2fx\ (cm^2)\ ; \qquad (28)$$

or

$$C = (e^4\lambda_o^5/4\pi m^2c^4\log_e 10)\ N^2f^2x\ (cm^2)\ ; \qquad (29)$$

or

$$C = (e^4\lambda_o^5/12m^2c^4\log_e 10)\ N^2f^2x\ (cm^2)\ . \qquad (30)$$

Consider the relative values between the pair of lines. From (28), (29), or (30), then, respectively,

$$C_1/C_2 = (\lambda_1/\lambda_2)^4\ (f_1/f_2) = 1.97\ , \qquad (31)$$

$$C_1/C_2 = (\lambda_1/\lambda_2)^5\ (f_1/f_2)^2 = 3.91\ , \qquad (32)$$

or

$$C_1/C_2 = (\lambda_1/\lambda_2)^5\ (f_1/f_2)^2 = 3.91\ , \qquad (33)$$

where the usual f-values have been substituted. The experimental ratios (Table II) have a mean of 2.07. Since no systematic deviations with the density N can be detected, it would appear that the theory of (31), with respect to relative f-values, is approximately correct over the entire pressure range. Accordingly, (32) and (33) are not confirmed. Hence it would seem that the f-value appearing in (26) and

(27) is superfluous.

Consider then, simply, equation (28). It yields

$$C_1/N^2f_1x = C_2/N^2f_2x = \text{const.} \qquad (34)$$

(The relative dependence of the components upon wavelength is small, and so is ignored for the moment). That (34) is in fact correct, is seen from the last two columns of Table II. (The variation with temperature because of the velocity factor in (28), is also ignored for the present).

The dependence upon x may be judged from the mean given for each tube length; it would seem, then, within the limit of error, to be that predicted by theory. (Some difference in the mean value for each tube length is to be expected, since each corresponds to a different contact of the thermocouple with the absorption cell).

The dependence upon N is best seen graphically. From (34),

$$\log (C_1/Nf_1x) = \log (C_2/Nf_2x) = \log N + \text{const.}*$$

A plot of either of the first two quantities against log N should yield a straight line with unit slope. This is strikingly illustrated in Fig. 8. The pressure range covered varies by a factor of 12,600 (7,400 in N). The observed deviations from linearity are thought to be within the

*This equation applies to the other two theories as well, if the f-value in (26) and in (27) be omitted.

limit of observational error. It would be rather difficult to construe the slope of the best straight line through the points as having a value of 1/2 or of 2, such as would be necessary to obtain agreement with those observers who found the half-breadth proportional to $N^{\frac{1}{2}}$, or to N^2.

At very low pressures, where radiation damping overshadows pressure broadening, (22), together with (23) and (24) yields

$$\log (C_1/Nf_1x) = \log (C_2/Nf_2x) = \text{const.}$$

This value of the ordinate is indicated by the horizontal line in the lower left hand corner of Fig. 8. The temperatures used in obtaining the spectrograms were presumed to include this lower pressure domain, in order that the already experimentally established natural breadth could be verified. However, it was found that this was precluded when the temperatures were subsequently determined (raised) according to the "in situ" calibration of the thermocouple. A plot of points corresponding to this low pressure region would presumably fall on the indicated horizontal line. The intersection point of the horizontal line with that one of unit slope, corresponds to a pressure of about 10^{-3}mm Hg*.

*This is not thought to be in serious disagreement with those observers who, starting at very low pressures and working up, found that their values of the half-breadth showed deviation from constancy at somewhat higher pressures (usually somewhere between 10^{-3} and 10^{-2} mm Hg), for the following reason. Because of the observational error, the precise determination of the pressure at which "deviation" from the horizontal sets in, is not possible. Furthermore, it depends considerably upon the subjective attitude of the experimenter. Thus, a

2. Absolute Values

For the numerical calculation involved in determining absolute values, see Appendix IV. There it is shown that the mean observed half-breadths are larger than those predicted by the theory of equation (26) by a factor of $3.09/f_1$ and of $2.95/f_2$, for the short and for the long wavelength component, respectively. The factors $1/f_1$ and $1/f_2$ result from that (apparently superfluous) f-value appearing in (26). If they are omitted, then experiment gives a value of the half-breadth of about three times that of theory; if they are included, the discrepancy is not only greater, but is different for each component. Since (26) differs from (27) only by a factor of $2\pi/6$, similar conconclusions apply to the theory of the latter equation. This disagreement is not surprising in view not only of the errors of the observation, but the assumptions of the theory.

The interaction distance of the Lorentz theory, computed from the mean value of C/N^2fx, is $\rho=201A$. This is in agreement of the result estimated by Korff, but is a little higher than that by other observers. According to the theory, $\rho \sim \bar{v} \sim T^{\frac{1}{2}}$. This dependence upon temperature cannot be verified, for the range used would change γ only by a factor of 1.3 at the extreme temperatures. For convenience, the mean value, $T = 560^{\circ}$ K, was used for determining ρ.

---

reading such as that for the lowest pressure shown in Fig. II (Plate 44), though definitely appearing to lie on the straight line with the unitslope, might readily be construed to lie on the horizontal line by an observer working up from the region of very low pressures. (The points correspond to γ equal to 1.3 times γ-natural breadth, about). Thus, the latter might well report a "deviation" at a pressure considerably above 10^{-3} mm Hg).

3. Some Prior Results

In Table III and in Fig. 9, is given similar data from some preliminary work. The relative values are in approximate agreement with the results discussed above, but the absolute value of the half-breadth are, on the average, one-half again as large.

The explanation of the latter is as follows. The half-breadths for the plates of Table II were, in the first instance, found to be consistently higher than those for Table III. At the suggestion of Dr. Houston, the thermocouple used for the final set of observations was calibrated "in situ" by the method described above. The "corrected" temperatures then yielded the results given in Table II, with half-breadths now lower than those of Table III. Since the thermocouple used for the earlier set had been damaged, it was not possible to calibrate it by the same method. However, a similar temperature "correction" would presumably, have brought the two sets of results into harmony. It is to be noted that, because of the nature of the vapor pressure curve, the relative dependence of the results upon N is little affected by a temperature correction proportional to the temperature above room temperature. This, then, must account for the linearity shown in Fig. 9.

TABLE III

Pl. No.	T(°K)	p(mm)	N	C_1 (cm^2)	C_2 (cm^2)	$\frac{C_1}{C_2}$	$\frac{C_1}{N^2 f_1 x}$ x10^{47}	$\frac{C_2}{N^2 f_2 x}$ x10^{47}
				Tube Length 3.90 cm				
16	423	5.01×10^{-4}	1.15×10^{13}	3.35×10^{-20}	1.09×10^{-20}	3.07	9.70	6.31
17	439	1.22×10^{-3}	2.70	9.62	3.29	2.92	5.06	3.46
18	471	5.75	1.18×10^{14}	1.80×10^{-18}	7.31×10^{-19}	2.46	4.95	4.02
19	508	2.88×10^{-2}	5.50	2.01×10^{-17}	7.20×10^{-18}	2.79	2.55	1.83
20	525	5.49	1.01×10^{15}	7.23	3.07×10^{-17}	2.36	2.72	2.31
21	549	1.29×10^{-1}	2.28	3.12×10^{-16}	1.52×10^{-16}	2.05	2.30	2.22
22	586	4.17	6.91	2.58×10^{-15}	1.37×10^{-15}	1.88	2.07	2.20
23	619	1.05×10^{0}	1.65×10^{16}	1.90×10^{-14}	1.29×10^{-14}	1.47	2.68	3.63
				Tube Length 1.30 cm				
25	500	2.04×10^{-2}	3.96×10^{14}	9.08×10^{-18}	3.20×10^{-18}	2.84	6.63	4.67
26	513	3.55	6.71	1.19×10^{-17}	5.38	2.21	3.04	2.75
27	539	9.12	1.64×10^{15}	6.72	3.11×10^{-17}	2.16	2.87	2.66
28	569	2.51×10^{-1}	4.28	4.22×10^{-16}	1.70×10^{-16}	2.48	2.65	2.13
29	593	5.01	8.20	1.49×10^{-15}	1.00×10^{-15}	1.49	2.55	3.42
30	620	1.07×10^{0}	1.68×10^{16}	7.39	3.41	2.17	3.01	2.77
31	651	2.35	3.50	5.31×10^{-14}	2.92×10^{-14}	1.82	4.98	5.48

4. Conclusion

No attempt has been made to estimate the experimental error; it is surely large. The principal uncertainty lies in the photographic photometry, in the vapor pressure equation, and, as to absolute values, in the determination of the temperature. Three (numerical) figures have been used throughout; no significance can be attached to the last one.

It is suggested that any future experiment involving an absorption cell gives attention to the following circumstance. A small side tube is connected to the cell. Within it reposes the supply of the absorbing substance. The cell is warmer than the side tube. The temperature of the latter determines the vapor pressure; that of the former serves to avoid condensation upon the windows. The thermocouple is securely attached to the side tube by fusion of a metal of high melting point. The seal of the windows is adequate to avoid leakage.

The success of the MgO windows paves the way for a number of interesting experiments. Still higher pressures are possible. This would permit a low-dispersion stigmatic spectrograph; hence, the plates could be calibrated by means of a rotating sector at the slit, and plates of uniform sensitivity could be used. The principal series of the alkalis bear investigation. The contour of a potassium line broadened by sodium is of interest[6]. Absolute trans-

ition probabilities of many a low vapor-pressure metal could be determined.

VIII. ACKNOWLEDGEMENTS

The author wishes to express his considerable indebtedness to Dr. D. S. Hughes, who constructed the bulk of the apparatus and otherwise laid the foundation for this work; to Dr. R. T. Brice, who developed the all important MgO windows; and to Dr. I. S. Bowen for his ever solicitous guidance.

IX. BIBLIOGRAPHY.

1 A. Einstein, Phys. Zeits. 18,121(1917).

2 R. C. Tolman, Phys. Rev. 23,693(1924).

3 R. Ladenburg, Zeits. f. Physik 4,451(1921); R. Ladenburg and F. Reiche, Naturw. 11,596(1923); Ch. Füchtbauer, Phys. Zeits. 21,322(1920).

4 S. A. Korff and G. Breit, Rev. Modern Physics 4,471(1932).

5 V. Weisskopf, Physik. Zeits. 34,1(1933).

6 H. Margenau and W. Watson, Rev. Modern Physics 8,22(1936).

7 The dispersion problem appears to have been attacked with this method, in the preceding century, by a number of persons independently. For its complete formulation, see Drude, Theory of Optics (1929), p. 382.

8 M. Planck, Berliner Ber. 1902,470; 1902,487; 1903,480; 1904,740.

9 For both the general formulation, and the application to radiation damping, see references 5 and 6. For the theory of the Fourier integral, see, for example, G. Joos, Theoretical Physics (1934), Chapter II.

10 V. Weisskopf and E. Wigner, Zeits. f. Physik 63,54(1930).

11 F. Hoyt, Phys. Rev. 36,860(1931).

12 R. Minkowski, Zeits. f. Physik 36,839(1926).

13 W. Voight, Munch. Ber. 1912, p. 603.

14 P. Debye, Physik. Zeits. 20,160(1919).

15 J. Holtsmark, Ann. d. Physik 58,577(1919).

16 See H. Margenau and W. Watson. Rev. Modern Physics 8,22(1936); references 7 to 13 incl.

17 J. Holtsmark, Zeits. f. Physik 34,722(1935).

18 J. C. Slater, Phys. Rev. 25,395(1925).

19 H. A. Lorentz, Proc. Amst. Acad. 8,591(1906); Handbuch der Physik (H. Geiger and K. Scheel) XX(1928), p. 522.

20 V. Weisskopf, Zeits. f. Physik 75,287(1932); see also reference 5.

21 O. Oldenberg, Zeits. f. Physik 47,184(1928); 51,605(1928).

22 H. Margenau, Phys. Rev. 48,755(1935); see also references 5 and 6.

23 W. Lenz, Zeits. f. Physik 80,423(1933).

24 H. A. Lorentz, reference 19;
W. Lenz, Zeits. f. Physik 25,299(1924);
H. Kallmann and F. London, Zeits f. Physik Chemie B2,207(1929);
V. Weisskopf, Zeits. f. Physik 75,287(1932);
H. Kuhn, Phil. Mag. 28,987(1937).

25 M. Kulp, Zeits. f. Physik 79,495(1932); 87,245(1933);
H. Margenau, Phys. Rev. 40,387(1932); 43,129(1933); 44,931(1933); 48,755(1935).

26 W. Lenz, Zeits. f. Physik 25,299(1924); H. Kallmann and F. London, Zeits. f. Physik Chemie B2,207(1929);
V. Weisskopf, Zeits. f. Physik 75,287(1932);
J. Holtsmark, Zeits. f. Physik 34,722(1925);
J. Frenkel, Zeits. f. Physik 59,198(1930);
L. Mensing, Zeits. f. Physik 61,655(1930).

27 See reference 5, and H. Margenau, Phys. Rev. 48,755(1935).

28 See, for example, V. Weisskopf, Zeits f. Physik 75,287(1932).

29 J. J. Hopfield, Astrophys. J. 72,133(1930).

30 For complete details as to both theory and experiment for the case of broadening by foreign gases, see references 5 and 6.

31 S. A. Korff, Astrophys. J. 76,124(1932); Phys. Rev. 38,477(1931).

32 M. Weingeroff, Zeits. f. Physik 67,679(1931).

33 W. Schütz, Zeits. f. Physik 45,30(1927).

34 G. R. Harrison and J. C. Slater, Phys. Rev. 26,176(1925);
G. R. Harrison, Phys. Rev. 25,768(1925).

35 B. Trumpy, Zeits. f. Physik 34,715(1925);
40,594(1926).

36 F. Waibel, Zeits. f. Physik 53,459(1929).

37 W. Orthmann and P. Pringsheim, Zeits. f. Physik 46,160(1927).

38 H. Becker, Zeits. f. Physik 59,583(1930).

39 See, for example, S. A. Korff, Astrophys. J. 76,124(1932), p. 130.

40 W. E. Forsythe and A. G. Worthing, Astrophys. J. 61,146(1925).

41 J. Strong and R. T. Brice, J.O.S.A. 25,207(1935).

42 Mack, Stehn, and Edlen, J.O.S.A. 22,245(1932).

43 B. O'Brien and V.L. Parks, Phys. Rev. 41,387(1932);
J. H. Webb, J.O.S.A. 23,157 and 316(1933).

44 See, for example, Lloyd A. Jones, Photographic Sensitometry (1934), p. 64.

45 J. C. Slater, Phys. Rev. 25,783(1925).

46 R. Ladenburg and F. Reiche, Ann. d. Physik 42,181 (1913).

47 For a possible explanation of this latter, see H. Kuhn, Zeits. f. Physik 76,782(1932).

48 See reference 42, and
D. L. MacAdam, J.O.S.A. 23,178(1933);
G. H. Dieke, J.O.S.A. 23,274(1933);
Kayser, Handbuch der Spectroscopie, Vol. 1(1900), p. 450;
D. C. Stockbarger and L. Burns, J.O.S.A. 23,379(1933);
J. R. Nielsen, J.O.S.A. 20,701(1930);
O. Oldenberg, J.O.S.A. 22,451(1932);
P. H. van Cittert, Zeits. f. Physik 65,547(1930).

49 See references 43, 44 and
G. R. Harrison, J.O.S.A. 19,267(1929); 24,59(1934);

Dobson, Griffith, and Harrison, Photographic Photometry (1926);
C. E. K. Mees, J.O.S.A. 23,229(1933);
Carroll and Hubbard, Bur. Stand. J. Res. 10,211 (1933);
R. Clark, Phot. J. 65,76(1925);
Bloch and Horton, Phot. J. 68,352(1928).

APPENDIX I

On the value of C' in (20)

To the extent that the Lorentz collision theory may be taken literally, it can be shown that the maximum value of the absorption coefficient is independent of N, and is of the order of several thousand. Hence it is manifestly impossible to determine $(\alpha x)_{max}$ $(=(\log_e 10)/C')$ from values of αx less than about 2.3 (Fig. 2). This is the reason, then, that absolute transition probabilities $(f = (C/C')^{\frac{1}{2}})$ cannot be obtained by this method.

Of course, in the radiation damping region, $(\alpha x)_{max}$ is smaller, falling off linearly with N. But pressures of less than 10^{-5} mm Hg would be required. And then the question of resolving power would enter. In the present experiment, even at the pressures used, this last consideration results in an apparent appreciable transmission at the center of the lines.

These remarks do not apply to the case of broadening by dissimilar atoms. There, since $(\alpha x)_{max} \sim N/N'$, and $(\delta\lambda) \sim (NN')^{\frac{1}{2}}$, where N' is the number of foreign particles, it is possible by a judicious choice of N and N' to have the maximum value of the absorption coefficient small, and still have an appreciable line width.

APPENDIX II

Area method.

The area A under the transmission curve is

$$\tfrac{1}{2}A = \int_0^\infty (1 - e^{-((C \log_e 10)/\delta\lambda^2)})\, d(\delta\lambda).$$

Substituting $y^2 = ((C \log_e 10)/\delta\lambda^2)$,

$$A/2(C \log_e 10)^{\frac{1}{2}} = \int_0^\infty (1 - e^{-y^2})/y^2\, dy.$$

Integrating the second term by parts, the integral turns out to be equal to $\sqrt{\pi}$ Thus

$$C = (A^2/4\pi \log_e 10) = 3.46 \times 10^{-18} A^2 \ (\text{Å}^2).$$

For a discussion of the Doppler effect, see reference 12.

APPENDIX III

Overlapping

For two lines of "strengths" C_1 and C_2,

$$I/I_o = e^{-\alpha x} = e^{-[C_1 \log_e 10/(\delta\lambda_1)^2 + C_2 \log_e 10/(\delta\lambda_2)^2]}, \qquad (1)$$

where $\delta\lambda_1 = (\lambda - \lambda_1)$; $\delta\lambda_2 = (\lambda - \lambda_2)$, $(\lambda_1 < \lambda_2)$. Then

$$1/\log_{10} I_o/I = 1/[C_1/(\delta\lambda_2 + d)^2 + C_2/(\delta\lambda_2)^2], \qquad (2)$$

where $d = (\lambda_2 - \lambda_1)$. If $R = C_1/C_2$, $y = \delta\lambda_2/d$, then

$$(C_2/d^2)/\log_{10} I_o/I = 1/[R/(1+y)^2 + 1/y^2].$$

For $|y| < 1$,

$$(C_2/d^2)/\log_{10} I_o/I = y^2/[1 + R(y^2 - 2y^3 + \ldots)]. \qquad (3)$$

For $|y| > 1$,

$$(C_2/d^2)/\log_{10} I_o/I = y^2/[1 + R(1 - 2/y + 3/y^2 - \ldots)]. \qquad (4)$$

A plot of $(C_2/d^2)/\log_{10} I_o/I$ against y^2 is as follows: for positive values of y, the curve leaves the origin asymptotically to a straight line through the origin of slope +1, approaching asymptotically, for $y \gg 1$, a straight line through the origin of slope y^2: $(C_2/d^2)/\log_{10} I_o/I = (1+R)$. For negative values of y, the curve leaves the origin asymptotically to a line through the origin of slope -1, but reaches a maximum value of $(C_2/d^2)/\log_{10} I_o/I$ at $y = -1/(1+R^{1/3})$, falls to a minimum at $y = -1$, then rises asymptotically to a line through the origin of slope $-(1+R)$. (A plot is not given because of the inherent difficulty of making a scale drawing).

(3) shows quantitatively the effect of the overlapping of line 1 on line 2. The "correction" term is $R(y^2 - 2y^3 + \ldots)$, a quantity increasing with y, but less rapidly so for positive values of y (series of alternating terms).

Similar conclusions apply for the overlapping of line 2 on line 1, where $d \to -d$, $y \to -y$ (now referred to λ_1), $C_2 \to C_1$, $R \to 1/R$, remembering that y is positive towards the overlapping line.

A change of procedure is suggested from (4), for $y \gg 1$, where the curves go asymptotically to straight lines through the origin of slopes $\pm(1+R)$, i.e., act like a single line of "strength" $C_2(1+R) = (C_1 + C_2)$. Choose as origin, the point λ_0, such that $(\lambda_2 - \lambda_0)/(\lambda_0 - \lambda_1) = R$, i.e., $\lambda_0 = \lambda_1 + d/(1+R)$. This, then, is a point intermediate to the two lines as determined by their "weights". Then

$$\delta\lambda_1 = (\lambda - \lambda_1) = (\lambda_0 - \lambda_1) + (\lambda - \lambda_0) = \delta\lambda_0 + d/(R+1),$$
$$\delta\lambda_2 = (\lambda - \lambda_2) = (\lambda - \lambda_0) - (\lambda_2 - \lambda_0) = \delta\lambda_0 - Rd/(R+1).$$

Substituting in (2), then, for $z = (\delta\lambda_0)/[Rd/(R+1)]$,

$$\left[(C_1 + C_2)/[Rd/(R+1)]^2\right] / \log_{10} I_0/I$$

is equal to

$$z^2 / \left[[R/(R+1)]/(1+1/Rz)^2 + [1/(R+1)]/(1-1/z)^2\right],$$

or, for $R \geq 1$ (i.e., $C_1 \geq C_2$), and if $|z| > 1$, is equal to

$$z^2/\left[1 + (3/R)(1/z^2) + (4(R-1)/R^2)(1/z^3) + (5(R^2-R+1)/R^3)\ (1/z^4) + \ldots\right]. \qquad (5)$$

Except for the "correction" term, this is the equation of a single line having a "strength" $(C_1 + C_2)$. The "correction" is greater for positive values of z than for negative ones. As a first approximation, the line is symmetrically broadened.

For partial overlapping, for the outer wing of the short wavelength line, from (3), assuming a priori $C_1 = 2C_2$, then for an error factor of 1.1 ± .09, measurements must be taken at $(\delta\lambda_1)^2/d^2 < .2$, i.e., $|\delta\lambda_1| < .45d$ (=15A). Thus, since the minimum value of $\log_{10} I_o/I$ for the usable part of the transmission curve is approximately .1, the maximum permissible width line that may be measured within this error is given approximately by $C_1 = (15)^2 \times 10^{-16} \times .1 = 2 \times 10^{-15}$ cm^2. (The error for the outer long wavelength wing would be double the above. For both inner wings, the corresponding error would be larger).

For nearly complete overlapping, for the short wavelength wing, from (5), assuming a priori $C_1 = 2C_2$, then, for an error factor of 1.1 ± .02, measurements must be taken at $d^2/(\delta\lambda_o)^2 < .15$, i.e., $|\delta\lambda_o| > 2.6\ d$ (=88A). As for above, the corresponding <u>minimum</u> is $(C_1 + C_2) = (88)^2 \times 10^{-16} \times .1 = 8 \times 10^{-13}$ cm^2. (The error for the long wavelength wing would be greater).

Thus, so long as $C_1 < 2 \times 10^{-15}$ cm^2, or $(C_1 + C_2) > 8 \times 10^{-13}$ cm^2, the error resulting from using the measured slopes is less than about 10%. In the intermediate cases (Plates 41, 42, 43; Table II), error is reduced by using the more favorable part of the wing.

In any case, the value of C_1 or of $(C_1 + C_2)$ will lie between C_1 and $(C_1 + C_2)$, and so the maximum error is 50%. Similarly, for the long wavelength wing, the error is 200%.

The predicted departure from linearity over the usable range of a line, if it existed, was masked by the errors of the photometry.

APPENDIX IV

Numerical Calculation Of Absolute Values

1. The ratio of experimental half-breadths to that of (26):

From (22),

$$\gamma = (2\pi \log_e 10)\, C/\varsigma \quad (\text{cm}).$$

Substituting for ς from (23),

$$\gamma/N\lambda_o^3 = (2mc^2 \log_e 10/e^2)\,(1/\lambda_o^5)\,(C/N^2 fx) \quad (\text{cm}).$$

Using

$$C_1/N^2 f_1 x = 2.23 \times 10^{-47} \quad (\text{cm}^7); \quad \lambda_1 = 7665 \times 10^{-8} \quad (\text{cm});$$

$$C_2/N^2 f_2 x = 2.18 \times 10^{-47} \quad (\text{cm}^7); \quad \lambda_2 = 7699 \times 10^{-8} \quad (\text{cm});$$

then, respectively,

$$\gamma_1/N\lambda_1^3 = 1.38 \times 10^{-13} \quad (\text{cm});$$

$$\gamma_2/N\lambda_2^3 = 1.32 \times 10^{-13} \quad (\text{cm}).$$

Comparing to

$$\gamma_{\text{theory}}/N\lambda_o^3 = (e^2/2\pi mc^2)\, f = 4.47\, f \times 10^{-14} \quad (\text{cm}),$$

it follows that

$$\gamma_{\text{exp.}}/\gamma_{\text{theory}} = 3.09/f_1 \; ; \; = 2.95/f_2 \; .$$

2. Lorentz collision diameter:-

From (13), and from (22),

$$\varsigma^2 = c\gamma/N\bar{v}\lambda_o^2 = (2\pi c \log_e 10/N\bar{v}\lambda_o^2)\,(C/\varsigma) \quad (\text{cm}^2).$$

Substituting for ρ from (23) ,

$$\rho^2 = (2mc^3 \log_e 10/e^2\lambda_o^2\bar{v})\ (C/N^2fx) \quad (cm^2),$$

where, from (14) ,

$$\bar{v} = (16RT/\pi M)^{\frac{1}{2}} = 7.65 \times 10^4 \quad cm/sec.$$

($T = 560°K$, $M = 39.1$). Then ($\lambda_o = 7680 \times 10^{-8}$cm, $C/N^2fx = 2.20 \times 10^{-47}$ (cm^7))

$$\rho^2 = 4.04 \times 10^{-12}\ cm^2 \ ; \quad \rho = 201A.$$

Fig. 1

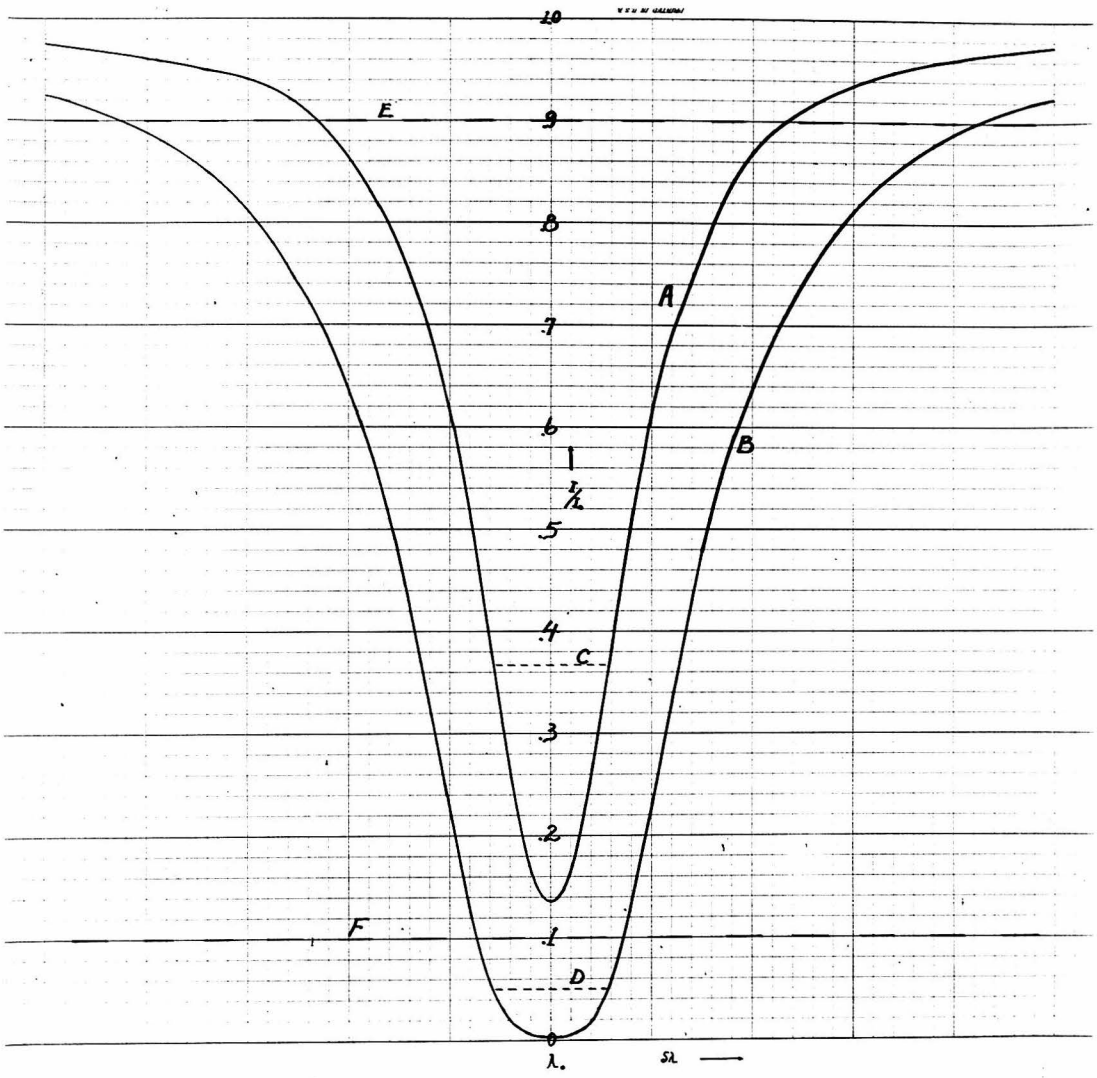

Fig. 2

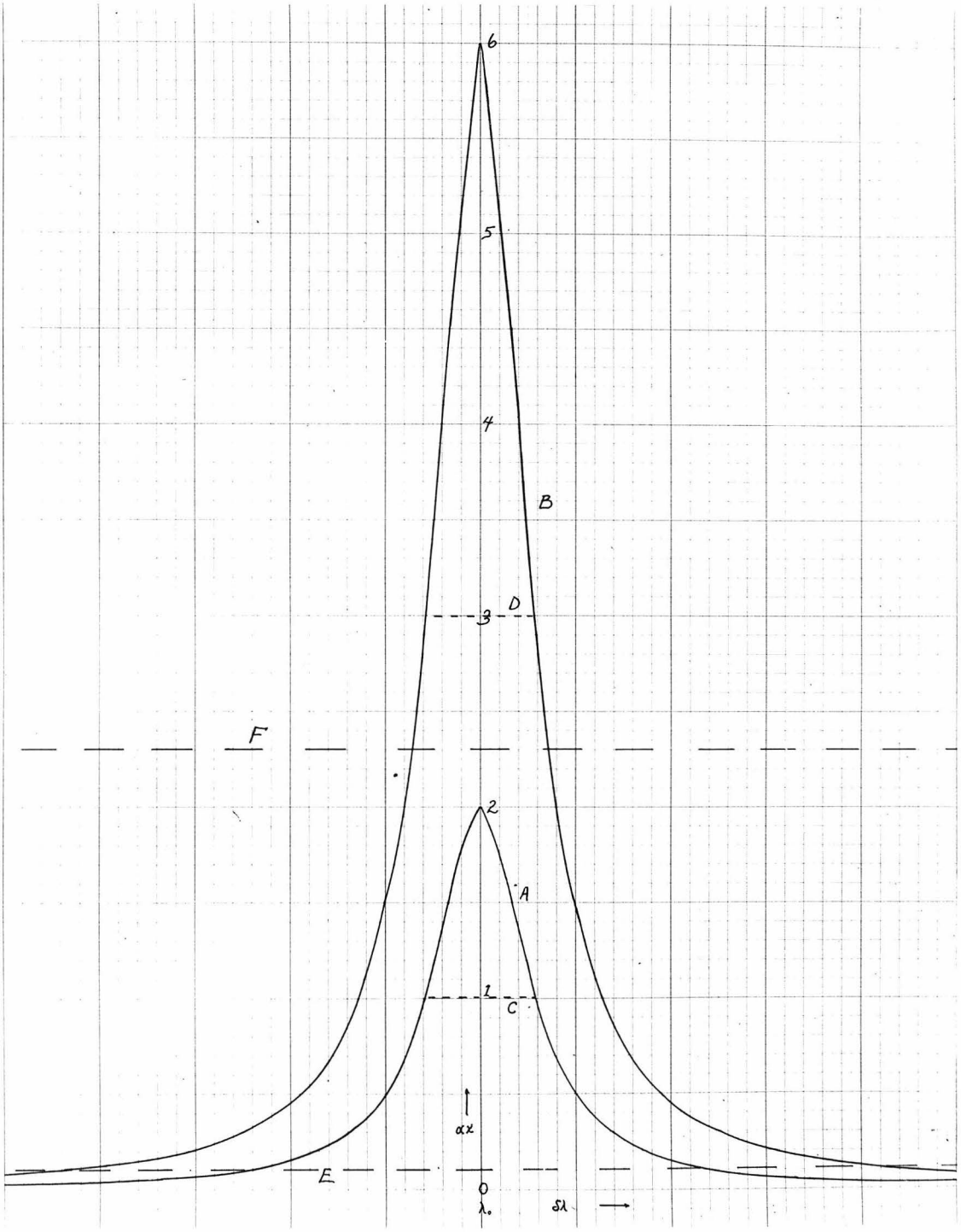

Fig. 3

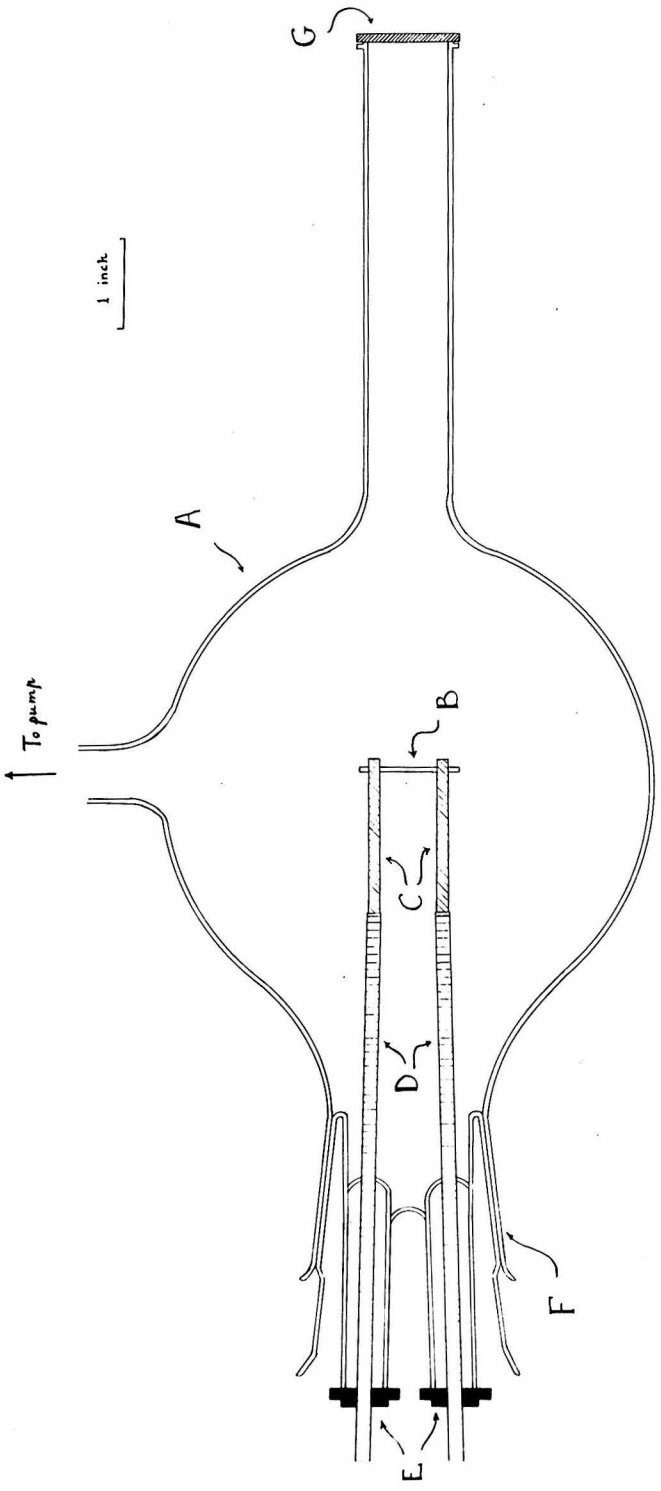

Fig. 4

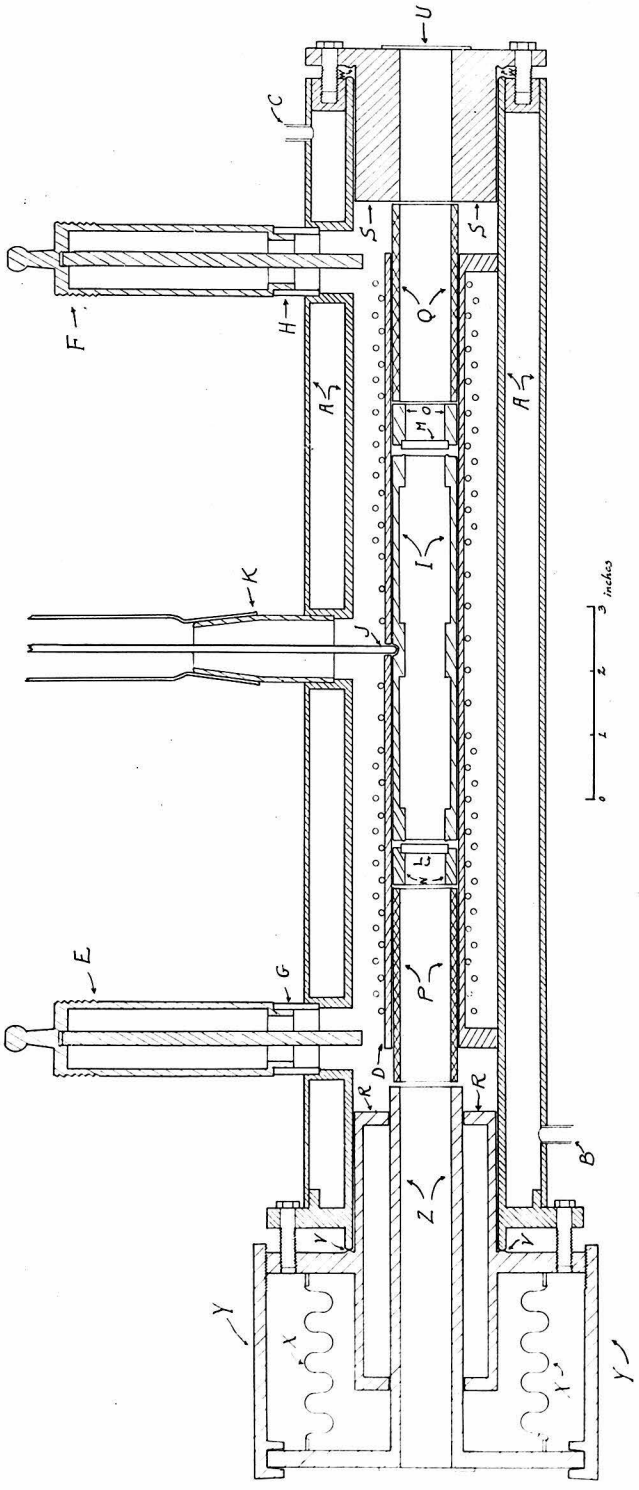

Fig. 5

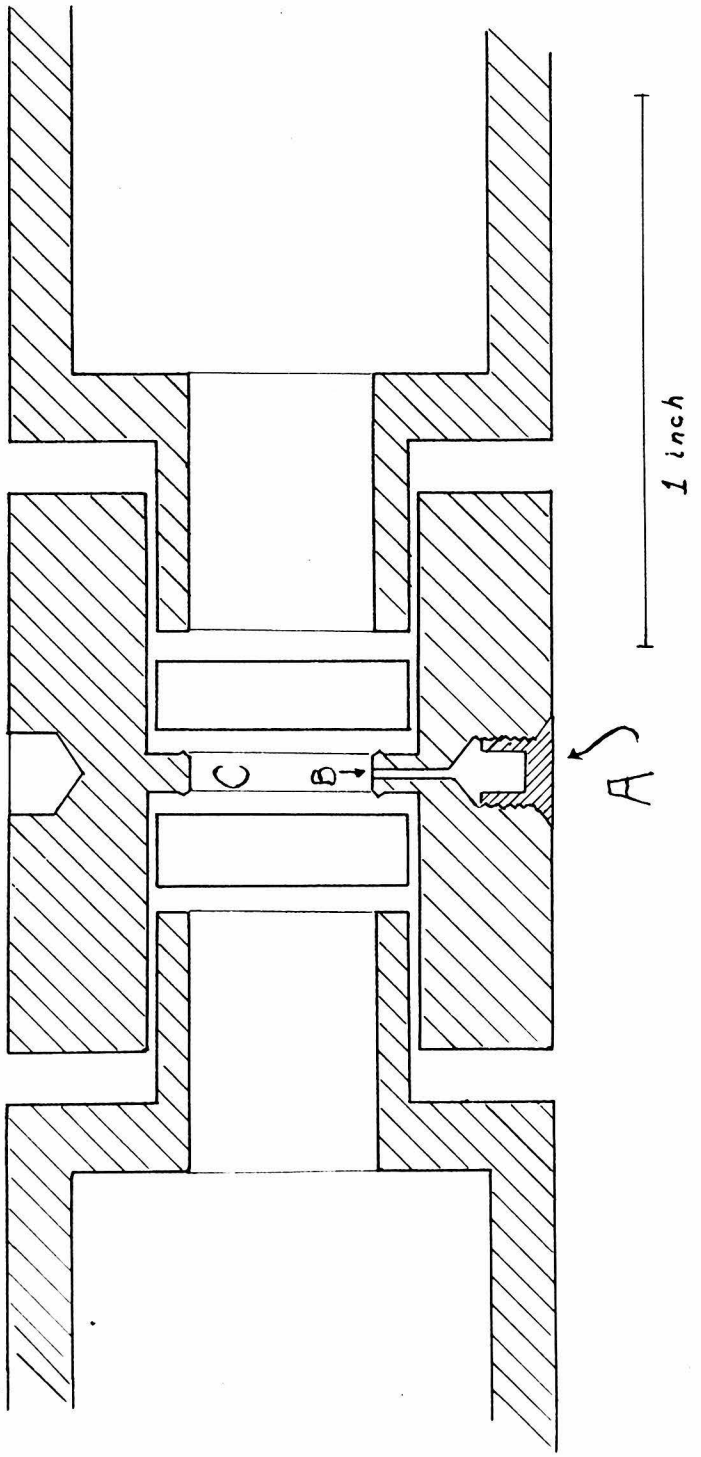

Fig. 6

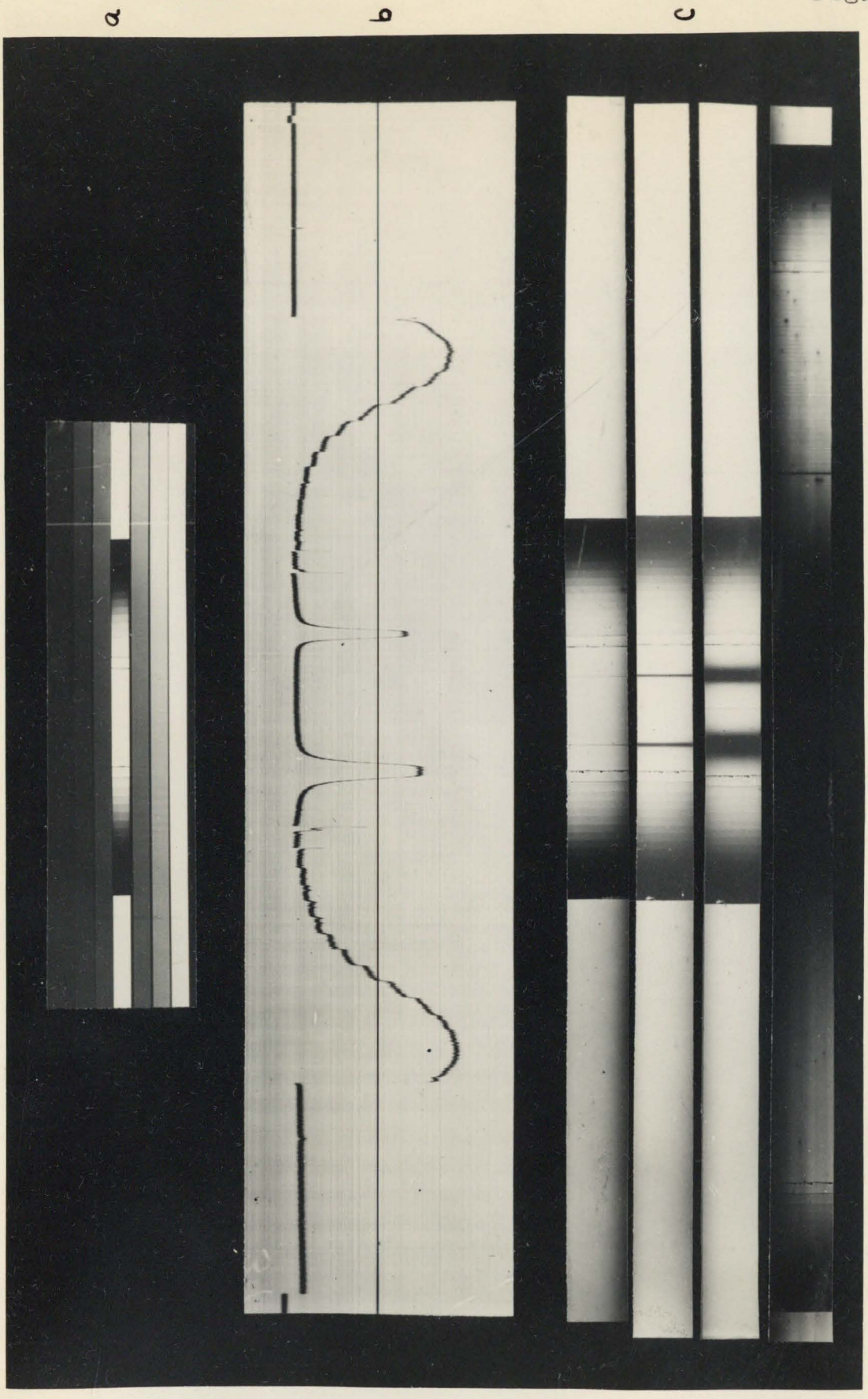

Fig. 7

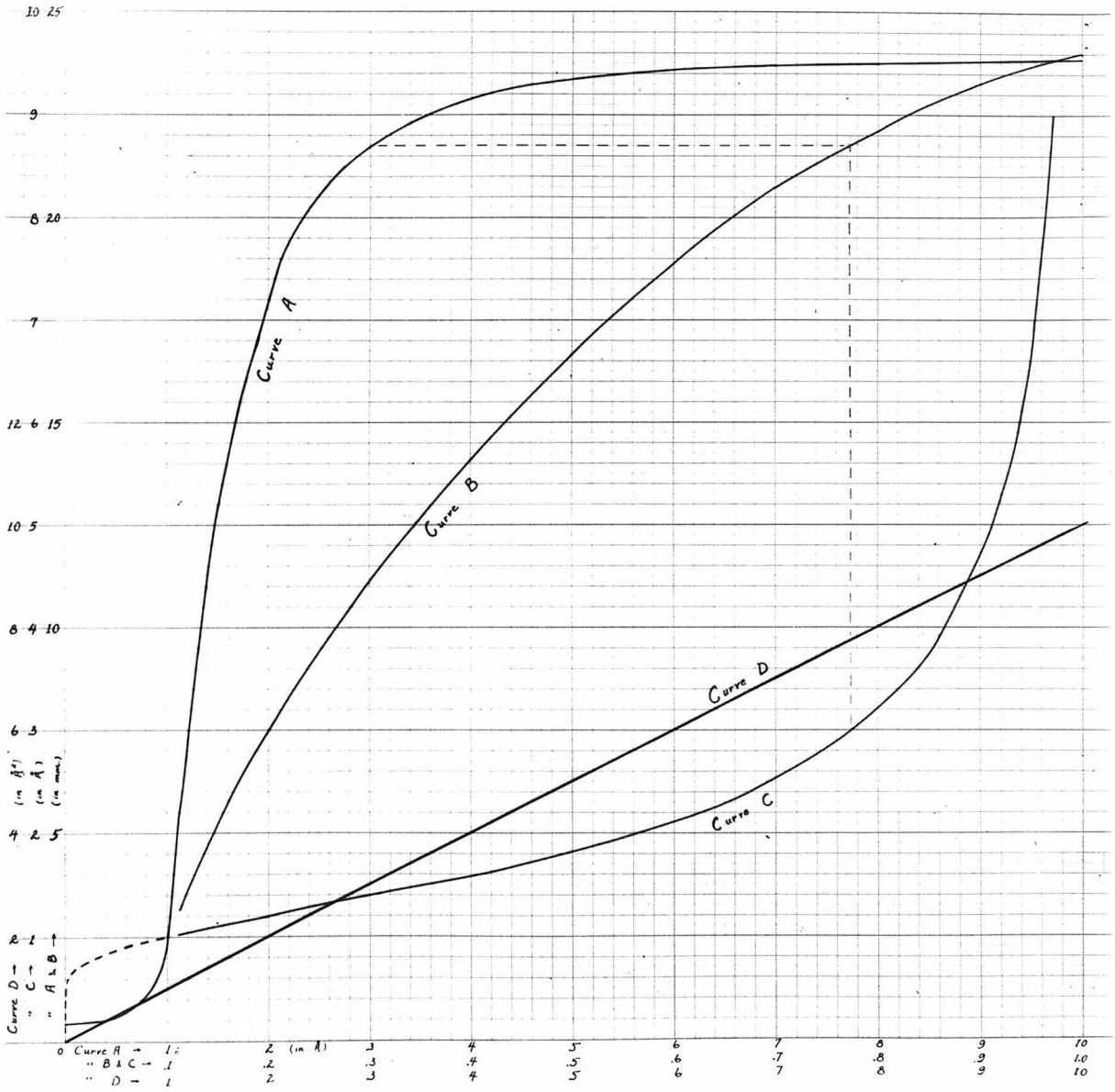
Curve A
Curve B
Curve C
Curve D
Curve D → (in Å⁻¹)
" C → (in Å)
" A & B → (in mms)
Curve A → 1
" B & C → .1
" D → 1
(in Å)

Fig. 8

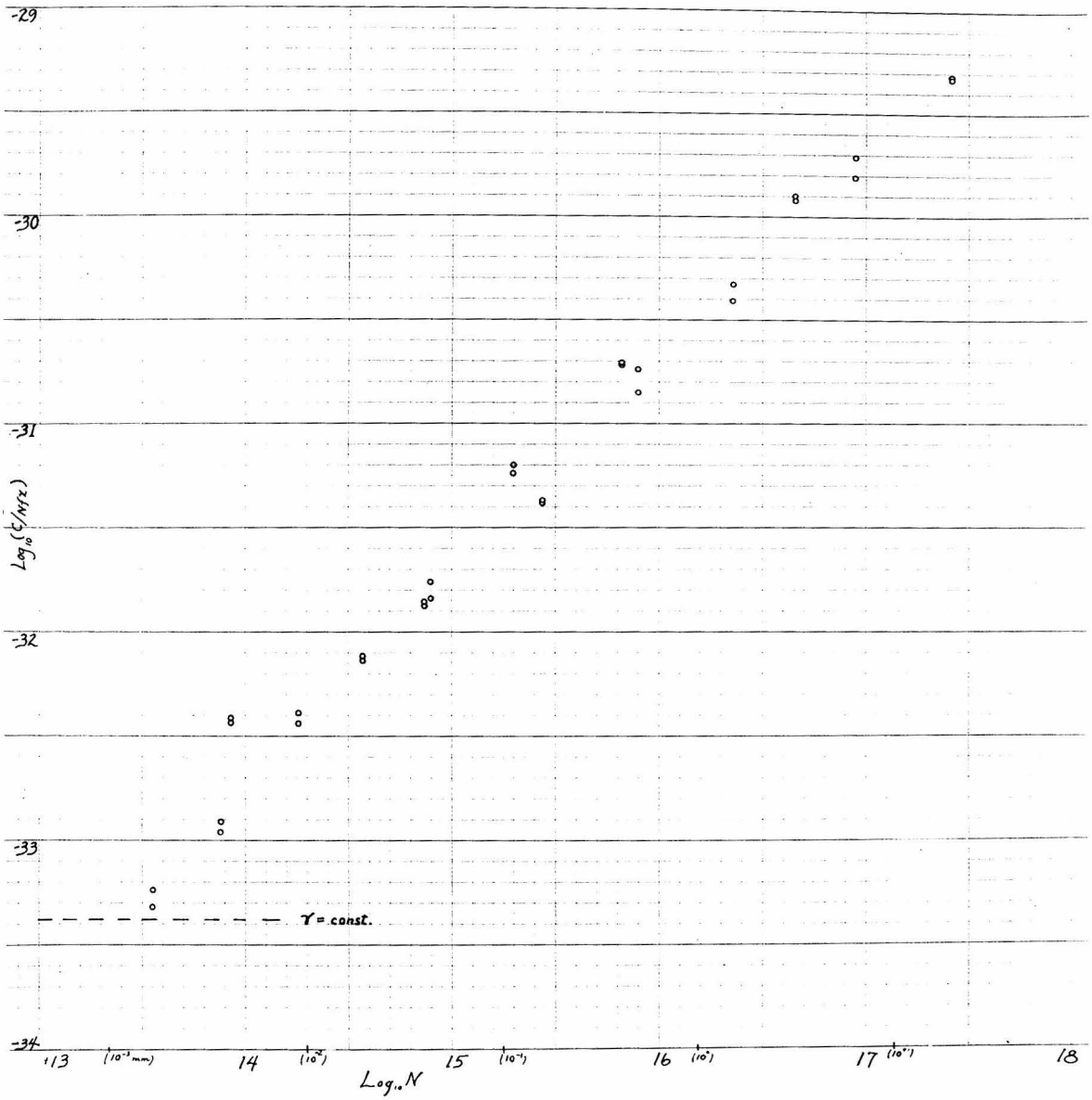
-29
-30
-31
-32
-33
-34
$\log_{10}(\xi/\mu m)$
γ = const.
13
(10⁻³ mm)
14
(10⁻²)
15
(10⁻¹)
16
(10⁰)
17
(10¹)
18
$\log_{10} N$

Fig. 9

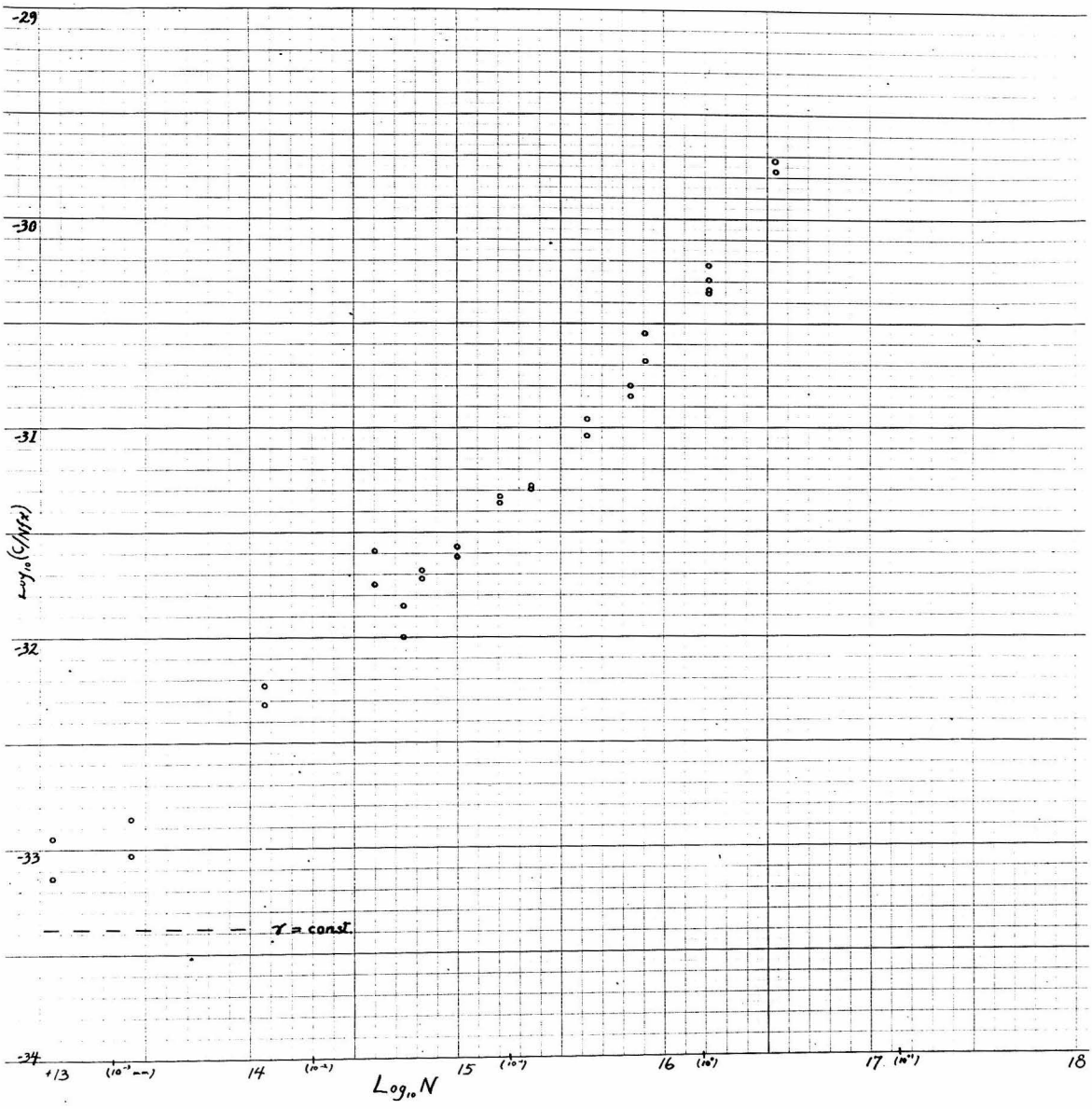
-29
-30
-31
-32
-33
-34
$\log_{10}(C/N\gamma z)$
— — — — — — — — γ = const.
+13
14
15
16
17
18
$\log_{10} N$